

ABSTRACT

Title of Document: SPATIAL AND TEMPORAL VARIABILITY
IN BENTHIC OSTRACODE
ASSEMBLAGES IN THE NORTHERN
BERING AND CHUKCHI SEAS, 1976 TO
2010

Laura Gemery, Master of Science, 2012

Directed By: Dr. Lee Cooper, University of Maryland
Center for Environmental Sciences

I examined living ostracode assemblages from the northern Bering Sea, collected between 1976 to 2010, and from the Chukchi Sea, collected in 2009 and 2010, to determine how climatic and oceanographic changes affect ostracode species distributions. I found the Bering Sea assemblage to be transitional in species composition between those inhabiting western Arctic continental shelves and the subarctic Gulf of Alaska. Temporal changes in the Bering Sea assemblage provide evidence that decadal temperature changes have affected species composition. For example, the proportion of *Normanicythere leioderma*, a predominantly Arctic species, decreased from 70% of the total assemblage population in 1999 to 15% by 2006. This decrease coincided with a shift in the Arctic Oscillation toward a positive mode and warmer Bering sea-surface temperatures beginning in the early 2000s. My results support the hypothesis that recent ocean temperature changes in the Bering-Chukchi Sea region are changing species composition in benthic ecosystems.

SPATIAL AND TEMPORAL VARIABILITY IN BENTHIC OSTRACODE
ASSEMBLAGES IN THE NORTHERN BERING AND CHUKCHI SEAS
FROM 1976 TO 2010

By

Laura Gemery

Thesis submitted to the Faculty of the Graduate School of the
University of Maryland, College Park, in partial fulfillment
of the requirements for the degree of
Master of Science
2012

Advisory Committee:
Dr. Lee Cooper, Chair
Dr. Thomas Cronin
Dr. Walter Boynton

© Copyright by
Laura Gemery
2012

Acknowledgements

I would like to thank my thesis committee, Dr. Lee W. Cooper, Dr. Thomas M. Cronin and Dr. Walter R. Boynton, for assistance and guidance in completing this thesis project.

Thanks to William Briggs, Jr. and Eugene Schornikov for meaningful discussions and identification regarding *Kotoracythere arctoborealis* vs. *Pectocythere janae*.

I greatly appreciate help from the many people who provided lab assistance, samples, data, graphics, and input on analyses and my manuscript: Alynne Bayard, Chris Bernhardt, Elisabeth Brouwers, Beth Caissie, Jesse Farmer, Ben Gordon, Jackie Grebmeier, Karin Lehnigk, Ronnie Lindsay, Rachel Marzen, Kristin McDougall, Han Nelson, David Reed, Christina Riesselman, Mike Torresan, and Moriaki Yasuhara. Zach Brown generously contributed sea surface temperature and sea-ice extent data.

Financial support was also provided in part by NSF ARC 0802290.

Table of Contents

Acknowledgements.....	ii
List of Tables.....	v
List of Figures	vi
Chapter 1: Environmental Factors Influencing Bering and Chukchi Sea	
Benthic Ostracodes.....	1
Introduction.....	1
Biogeography of Arctic and Subarctic Ostracodes.....	4
Environmental Factors Affecting Arctic and Subarctic Ostracode Abundance and Range.....	6
Detrended Correspondence Analysis (DCA) of ostracodes from the Bering, Chukchi, Beaufort, Laptev, and Kara Seas	6
Ocean Temperature	8
Salinity.....	11
Productivity.....	12
Primary Productivity and Species Diversity.....	14
Summary	16
Figures 1.1 – 1.12.....	18
Chapter 2: Temporal Changes in Benthic Ostracode Assemblages in the Northern Bering and Chukchi Seas from 1976 to 2010	
Introduction.....	31
Environmental Setting	32
Materials and Methods	35
Ostracode Sampling.....	35
Sample Processing	37
Sources of Temperature and Sea-ice Data.....	38

Statistical Analyses	39
Results	40
Bering Sea assemblage composition	40
Distributions of dominant taxa in the Arctic Ocean and North Pacific	41
Temporal trends in Bering Sea indicator species	42
Canonical correspondence analysis for Bering Sea species	44
Chukchi Sea ostracode assemblages	46
Discussion	46
Conclusions	48
Table	50
Figures 2.1 – 2.8	51
Appendices	60
References, Chapter 1	61
References, Chapter 2	74

List of Tables

Table 2.1. Listing of research cruises by year, month, ship, and region, from which samples for this study were collected.

List of Figures

Figure 1.1. Location of sediment samples used in the present study of benthic ostracodes and areas discussed in the text by year: Chukchi Sea, Bering Sea, Norton Sound, Chirikov Basin, Inner Shelf region off western Alaska, Alaskan Coastal Current.

Figure 1.2. Scanning electron photo of Arctic ostracode *Henryhowella* cf. *asperrima*, adult female, right valve (1.2A) and general anatomy of a Podocopid ostracode (1.2B). [Photo courtesy of Moriaki Yasuhara and illustration courtesy of David Horne as published in Horne et al., (2002)]

Figure 1.3. September (1.3A) and January (1.3B) sea-surface temperatures (SST) representing mean summer and winter temperatures, respectively. Maps are web-based products from the U. S. National Oceanic and Atmospheric Administration National Oceanographic Data Center (NODC): <http://www.nodc.noaa.gov/cgi-bin/OC5/PACIFIC2009/showclimatmap.pl>

Figure 1.4. Map showing locations of circum-Arctic continental shelf ostracode samples used in comparative biogeographic analysis of Bering and Chukchi Sea ostracode assemblages. Map derived from: <http://www.ngdc.noaa.gov/mgg/bathymetry/arctic/currentmap.html>

Figure 1.5. Detrended correspondence analysis (DCA) comparing Bering and ostracode assemblages with those from circum-Arctic shelves shown in Figure 1.4 (n=306, 43,200 specimens). This representation illustrates how ostracode assemblages in near-shore marine Arctic environments differ from northern Bering Sea assemblages. Colored circles represent sample locations: Bering (blue dots), Chukchi (red dots), Beaufort (green dots), Laptev (yellow dots), and Kara (black dots). “Bering A” sample group plots low on axis two and includes larger proportions of *N. leioderma* and *S. bradii*, while “Bering B” group contains larger proportions of *S. complanata* represented in 2006 and 2009 samples. There are no sharp boundaries among the samples; the gradations between the samples are due to differences in years collected and the geographically varied salinity and temperature regimes of the regions. (Samples with <20 specimens and samples with from water depths ≥ 200 m were excluded.)

Figure 1.6. Percent abundance and latitudinal distribution of circum-Arctic species *P. pseudopunctillata* and temperate species *P. janae* in the Bering Sea. *P. pseudopunctillata* is common only in the northern most Bering Sea near the Bering Strait (63-64°N latitude), where it likely migrates from the Beaufort Sea region. In contrast, the temperate species *P. janae* is primarily distributed near latitude 62°N, south of St. Lawrence Island where it presumably migrates north from the Gulf of Alaska during periods of warmth in the Bering Sea.

Figure 1.7. Abundance of *S. bradii* during three intervals showing the principal temperature control of its abundance. Samples are denoted by the blue dots on the respective maps, from relatively cold years of 1994 and 1999 (1.7A) and 2009 and 2010 (1.7C) show its abundance increases to sometimes 50-80% of the assemblage. In contrast, samples from the warm years of 2001-2006 (1.7B) show its abundance declines to <10% of assemblage in all but 2 samples.

Figure 1.8. Salinity in the Bering Sea and Norton Sound region in September 2009. Map derived from:

<http://www.nodc.noaa.gov/cgi-bin/OC5/PACIFIC2009/showclimatmap.pl>

Figure 1.9. Longitudinal distribution of *P. janae* and *C. macchesneyi* in the Bering Sea (1.9A), showing *P. janae* is most abundant in the southwestern part of the study region, while *C. macchesneyi* is abundant in the central and eastern (Norton Sound) regions. Longitudinal distribution of *S. complanata* (southwest region) and *P. pseudopunctillata* (Norton Sound) (1.9B). The latitudinal distribution of *S. bradii* and *N. leioderma*, the two most common species in the northern Bering Sea, shows that occur together and this reflects their eurytopic ecology (1.9C). Plots are based on 110 samples collected between 1976-2010 and having >10 total specimens in each sample.

Figure 1.10. Contour plots of distribution, depth and abundance of *P. pseudopunctillata* (1.10B) and *C. macchesneyi* (1.10C) along a transect of the of the northern Bering/Chukchi/Beaufort Sea (outlined in red) (1.10A, map). Transect runs from the northern Bering to Chukchi and then into the Beaufort Sea. Blue dots on map show a 700-surface-sample ostracode database combined with Bering Sea samples from the current study (Figure 1.1). The distributions of *C. macchesneyi* and *P. pseudopunctillata* appear to be influenced by the Alaska Coastal Current, which flows along the western Alaskan coast into the Chukchi and Beaufort Seas. The abundance *P. pseudopunctillata* is a dominant species along the coasts of the Chukchi-Beaufort Sea representing on average 40-80% of the assemblage. *C. macchesneyi* is common (>30% of assemblage on average) along the Chukchi-Beaufort shallow margins.

Figure 1.11. Summer sea-surface temperature (SST) from the Chirikov Basin and Inner Shelf regions (1.11A) plotted against percent abundance of *P. janae* and *N. leioderma* since 1998 (1.11B). Primary productivity in the Inner Shelf (1.11C) is plotted from 1988 to 2009. (SST and primary productivity data courtesy of Zach Brown as presented in Brown et al., 2011. I define the Inner shelf region (<50 m depth) to include the Eastern Bering shelf and the Gulf of Anadyr (bounded by Cape Navarin to the south, St. Lawrence Island to the east, and Cape Chukotskiy to the north.)

Figure 1.12. Percent abundance of *N. leioderma* (1.12A) and *P. janae* (1.12B) plotted as a least-squares fit regression against primary productivity as measured in the Inner shelf of the eastern Bering Sea. *N. leioderma* is significantly more abundant as productivity is reduced ($r^2=0.49$). In contrast, *P. janae* abundance is correlated with higher productivity ($r^2=0.63$).

Figure 2.1. Bathymetry of the Bering and Chukchi Seas. Map derived from: <http://www.pmel.noaa.gov/np/pages/seas/bseamap2.html>

Figure 2.2. Number of open water days (reflecting length of ice-free period) in the Chirikov Basin and along the Inner Shelf, 1979-2009. Trend line shows open water duration in the Chirikov Basin (north of St. Lawrence Island) has increased over these three decades, accounting for an ice loss of $\sim 77 \pm 37$ km² of ice per year, with ice exiting by mid-June (Brown et al., 2011). “Open water” is defined as a satellite-derived sea-ice concentration below 10%. The Inner shelf region (0–50 m depth) includes the Eastern shelf and the Gulf of Anadyr (bounded by Cape Navarin to the south, St. Lawrence Island to the east, and Cape Chukotskiy to the north); The Chirikov Basin region is bounded by St. Lawrence Island to the south, the Chukotka Peninsula to the west, Seward Peninsula to the east, and Bering Strait to the north.

Figure 2.3. Cluster analysis with a Euclidean similarity measure of 21 species

of ostracodes in the northern Bering Sea, 1976-2010. This grouping sorts species with similar patterns of abundance.

Figures 2.4A-C. Modern Arctic distribution and abundance of three key cryophilic species, *N. leioderma* (a), *S. bradii* (b), and *S. complanata* (c), based on a ~700-coretop sediment sample database (the Modern Arctic Ostracode Database, MAOD). The red circles indicate species presence, while the white circles indicate absence. The MAOD provides census data for approximately 100 species of benthic marine Ostracoda from modern surface sediments collected over the last 50 years from the Arctic Ocean and adjacent seas (Cronin et al., 2010).

Figure 2.4D. Contour plot of distribution, depth and abundance of *P. janae* along the red-outlined Chukchi/Beaufort Sea area. Transect runs from the Chukchi to the Beaufort Sea (left to right). From the MAOD 685-sample database, 140 samples (black circles) were analyzed for the abundance of *Pectocythere*. *P. janae* is rare along the Chukchi-Beaufort shelf, only appearing in 2 samples during 1969 and 1970 with an abundance of 5-18% of the sample's total ostracode population. It is absent along the Laptev-Kara shelf and is a more temperate Pacific species found in the Gulf of Alaska by Brouwers (1990).

Figure 2.5A. Chirikov Basin and Inner Shelf mean summer sea-surface

temperature (SST) from 1982 to 2009 (purple and green lines). In order to have a temperature record that encompassed the study's time period, we include May SST for the southeastern Bering since 1975 and summer BWT for the eastern Bering since 1982. Because the central-northern Bering Sea is shallow (<50m) and well mixed, SST and BWT patterns generally show broad decadal patterns but do not provide year- and site-specific temperature data for our exact study region or exact temperatures that ostracode species require. (Data from <http://www.beringclimate.noaa.gov/data/>) This graph also illustrates the correlation between the SST and BWT data, $R^2 = .723$ ($p < 0.05$).

Figures 2.5B-E. Plots of abundances of the four most common species in Bering Sea, 1976-2010. Results represent the relative abundance of the major taxa out of the entire population for each year. (Samples from the Norton Sound area in 1978 were removed from the plot, as they were located in a river plume area and are not representative of the central Bering area assemblage.) Confidence limits were generated using the binomial methods of Buzas (1990).

Figure 2.6. Canonical correspondence analysis (CCA) results of five dominant ostracode species frequencies ($n=77$) in relation to several environmental variables (sea-air temperature [SAT] in the Chirikov Basin, SAT along the Inner Shelf, the Arctic Oscillation Index, May sea surface

temperature [SST] in the southeastern Bering Sea) that may influence their overall abundance and distribution. The green vector lines show the environmental variables and the quadrant and samples with which they are associated. Although it is difficult to disentangle the independent effects of the variables, the CCA shows that *P. janae*'s ecology is distinct from the other dominant species and its frequency correlates with high SATs, indicating a warmer water affinity. Samples from the year 2010 (maroon circles) are in the opposite quadrant from the SAT vectors and *P. janae*, consistent with colder water temperatures in 2010. Samples from 1994 (light gray circles) cluster together indicating the dominance of *S. bradii* and *N. leioderma*, which, in that year, represented 36% and 49% of the total ostracode population, respectively. *C. macchesneyi*, a species that can tolerate reduced salinity, shows a correlation with a few samples from 1977 and 1976 (pink and moss green circles) that are located in lower salinity waters of Norton Sound. Samples from 2010 (maroon circles) also contained a higher percentage of *C. macchesneyi* compared to past years. Data corresponding to *N. leioderma* is centrally distributed in the plot, meaning that it is abundant in most of the samples in most of the years. According to the eigenvalues, axis one (80%) and axis two (15%) account for a combined 94% of the variance in this analysis.

Figure 2.7. The Chukchi Sea ostracode species assemblages in 2009 and 2010. Bar plots include species that comprised >1% of the total species

population. In 2009, eight samples yielded 361 ostracode specimens and in 2012, eight samples yielded 837 specimens.

Figure 2.8A-D. Contour plots comparing species abundance in cold years (1994 and 1999) vs. warm years (2001-2006) north and south of St. Lawrence Island. Maps (top) show central-northern Bering shelf study area and locations of samples (blue dots) in the years represented. Contour plots show abundance of key taxa in south-north cross sections to depict the changes in major species abundance during these ocean-atmosphere shifts. Two assemblages are present; one dominated by Arctic species (*N. leioderma* and *S. bradii*) in colder years, another with significant numbers of more temperate species (*P. janae*) representing a mixture of Arctic and sub-Arctic species.

Chapter 1: Environmental Factors Influencing Bering and Chukchi Sea Benthic Ostracodes

Introduction

During the past few decades, the Bering and Chukchi Seas have experienced increases in temperature, freshwater content, primary productivity (Chukchi Sea) and reductions in the length of the sea-ice season and primary productivity (Bering Sea), and overall changes in continental shelf ecosystem structure and carbon cycling (Grebmeier et al., 2006a, 2010, 2011; Grebmeier, 2012; Arrigo et al., 2011; Brown et al., 2011). Dramatic changes in ice extent have been observed in the Arctic Ocean (Stroeve et al., 2008), particularly north of the Bering Strait in the Chukchi Sea, where extreme sea-ice retreats from 2007 through 2009 lengthened the open-water season in fall by about four weeks (Grebmeier et al., 2010). Sea-ice loss has been especially significant along the Chukchi shelf margin (Steele et al., 2008). In the Chirikov Basin, in the northern Bering Sea (the shelf bounded by St. Lawrence Island to the south, the Chukotka Peninsula to the west, the Yukon Delta to the east and the Seward Peninsula and Bering Strait to the north) sea-ice cover has decreased significantly from 1979 to 2009, resulting in 25 more days of sea-ice-free open water (Brown et al., 2011).

Biological observations in these areas have documented changes in species composition and northward range extensions for zooplankton, bottom-dwelling organisms and fish that may collectively signify a large, climate-driven ecosystem reorganization (Mueter and Litzow, 2008; Grebmeier, 2012). In the Bering and Chukchi Sea region, ecosystem reorganization (also called a regime shift, Hare and Mantua, 2000; Bluhm and Gradinger, 2008) may be related to changing seasonal sea-ice conditions, which can alter benthic-pelagic ecosystem processes and cause a cascade of consequences through the food web (Grebmeier et al., 2006a). For example, the timing of spring sea-ice retreat from the continental shelf is thought to influence the timing of the spring phytoplankton bloom (Hunt and Stabeno, 2002; Hunt et al., 2002). Under this scenario, a longer ice season (later spring sea-ice retreat) causes an earlier ice-associated phytoplankton bloom, which in turn affects the vertical deposition of plankton debris to benthic ecosystems. In contrast, a shorter ice season (earlier spring retreat) is associated with a later spring phytoplankton bloom. A later bloom is better timed with zooplankton, which provide high grazing pressure on phytoplankton and, in turn, support higher trophic level secondary production at the expense of benthic species. Evidence for an ecosystem reorganization is also provided by biological restructuring of the composition and distribution of organisms, such as those observed in recent changes in Arctic benthic biodiversity, community composition, biomass, and range expansions (Bluhm and Grebmeier, 2011; Grebmeier, 2012).

This work is the first to analyze benthic ostracode assemblages from sediments of the northern Bering and Chukchi Seas. Samples were collected during a number of recent and prior research cruises extending back to the 1970s (Figure 1.1). Ostracodes, as meiobenthic, bivalved Crustacea, have several distinct advantages for retrospective ecosystem study. Their calcium carbonate shells are preserved in marine sediments enabling species identification from shell morphology, even after their soft parts decompose. An example of an ostracode carapace (Figure 1.2A) illustrates typical preservation states upon which identifications can be based. Chitinous appendages (Figure 1.2B) are commonly preserved when a specimen was alive at the time of collection (e.g. in a benthic grab sample). Unlike macrofaunal species, which cannot be enumerated quantitatively in sediment cores because of their size and scarcity, adult ostracodes range in size from 0.5 mm to 2 mm and can be quantified in small samples available from individual grab and/or core samples. Moreover, marine ostracode species have biogeographical and ecological limits controlled by temperature, salinity, or nutrient/food availability (Stepanova et al., 2007; Cronin et al., 2010a; Yasuhara et al., 2012b). Consequently, they have been used extensively in paleoecology and paleoclimatology to document climatically driven changes in ocean temperature, circulation, salinity, and ocean productivity (e.g. Cronin and Raymo, 1996; Didié and Bauch, 2000; Cronin et al., 1994, 2005, 2010b; Yasuhara et al., 2012a).

I describe here the environmental factors controlling the distribution of Bering and Chukchi Sea ostracodes, providing species-specific examples, based on new analyses of bottom samples. A chapter to follow (Chapter 2), more specifically analyzes temporal changes in ostracode assemblages and ocean temperature, with emphasis on the northern Bering Sea during the period 1976-2010. For this study, species assemblages were identified for 225 surface sediment samples from the northern Bering Sea collected from 1976-2010 and 16 from the Chukchi Sea sampled from 2009-2010 (Figure 1.1). Species percent abundances (proportion of total ostracode assemblage) were calculated for each sample from species census data (Appendix 1A and 1B).

Biogeography of Arctic and Subarctic Ostracodes

On large spatial scales, the latitudinal distributions of continental shelf ostracode species are controlled largely by ocean temperature requirements for survival and/or reproduction (Hazel, 1970). This is due to the fact that continental shelves are located above the permanent ocean thermocline (typically 30 to 200 m water depth in low latitude oceans), and experience seasonal temperature variability to which individual species are adapted. For example, along eastern North America, the largest temperature-controlled faunal transition in benthic invertebrates (including ostracodes) occurs near

Cape Hatteras, North Carolina where a steep ocean temperature gradient reflects the influence of the warm Gulf Stream flowing from the southwest and the cool shoreward current flowing from the north (Hazel, 1970). Ocean temperature also controls the distribution of ostracode species along the west coast of North America from Baja, California to the Gulf of Alaska (Valentine, 1976; Brouwers, 1988a, b). Because of these gradients, I also expected to observe community changes in the Bering Sea, where a fairly strong northwest-to-southeast surface temperature gradient also exists (Figure 1.3).

Ostracode species adapted to extremely cold temperatures inhabit circum-Arctic continental shelf regions. For the purposes of the following discussion, the term circum-Arctic refers to high latitude, northern hemisphere continental shelf regions (less than 100 m water depth) that include the Kara, Laptev, East Siberian, Chukchi, Beaufort and Bering Seas. Prior taxonomic, ecological and biogeographic studies of Arctic ostracodes include Sars (1866, 1922-28), Elofson (1941), Neale and Howe (1975), Joy and Clark (1977), Cronin (1981; 1988), Whatley (1982), Penney (1989), Hartmann (1992), Whatley and Coles (1987), Stepanova and colleagues (2003; 2004; 2006; 2007) and Schornikov and Zenina (2006). These data have been used in numerous paleoecological studies of the Arctic Ocean (e.g. Clark et al., 1990; Brouwers et al., 1991; Cronin et al., 1993, 1994, 1995, 2010b; Valentine, 1976; Brouwers 1988a, 1988b). This current study takes advantage of the temperature sensitivity of ostracode species to test whether their

disturbances reflect large-scale, climate-driven changes are occurring in the Bering-Chukchi region since the 1970s.

Environmental Factors Affecting Arctic and Subarctic Ostracode

Abundance and Range

Many physical, chemical and biological factors influence the distribution of benthic marine ostracodes both globally across climate zones and locally, within a particular region. In this chapter, I will first present a comparative biogeographic analysis of assemblages from Bering samples (Figure 1.1) integrated with previously documented assemblages from Arctic continental shelves (shown in Figure 1.4).

Detrended Correspondence Analysis (DCA) of ostracodes from the Bering, Chukchi, Beaufort, Laptev, and Kara Seas

A detrended correspondence analysis (DCA) was conducted using PAST (PAleontological Statistics; Hammer et al., 2001) to compare Bering Sea assemblages with those from circum-Arctic continental shelves. The multivariate DCA technique analyzes for similarities among samples based on species percent abundance. Correspondence analyses are commonly used to analyze similarities and dissimilarities among sample and species

relationships (Radi and deVernal, 2008; Park and Cohen, 2011). The first two axes of the DCA illustrate the similarities and differences between the Bering and Chukchi assemblages and those from other Arctic continental shelves (Figure 1.5). A total of 306 samples containing 43,220 ostracode specimens were used in the DCA. Samples with <20 specimens and samples with from water depths ≥ 200 m were excluded to limit the analysis to relatively shallow water depths.

The plot of the first and second principal components, which accounts for 51% of the variance, shows that Kara and Laptev Sea samples are similar in ostracode assemblage composition (Stepanova 2003; 2007), that most Beaufort (green circles) samples group separately from the Laptev and Kara Sea samples and that most Chukchi samples (red circles) group with Laptev-Kara samples or are intermediate between those from the Bering and Laptev-Kara Seas. Additionally, the plot indicates separation between two groups of the Bering Sea samples, hereafter termed “Bering B” and “Bering A” (Figure 1.5). Bering A samples plot low on axis two due to larger proportions of *Normanicythere leioderma* and *Sarsicytheridea bradii*. Together these two species comprised up to 94% of the total Bering Sea ostracode assemblage during colder years between 1976 and 2010 (Chapter 2). They were less common during years in which northern Bering Sea summer bottom temperatures were $>0-2^{\circ}\text{C}$. *S. bradii*, which reaches $>50\%$ of the community composition in the Bering Sea, was less common in the Chukchi Sea (27%

maximum in 2009 and 8.4% in 2010) as was *N. leioderma* (0.8% in 2009 and 11% in 2010). In contrast to the Beaufort Sea and Chukchi Sea where it is common (17% in 2009 and 16% in 2010; Chapter 2), *Paracyprideis pseudopunctillata* comprised only 2% of the total Bering Sea assemblage. The Bering B group contained larger proportions of *Semicytherura complanata* in samples collected in 2006 and 2009.

The DCA shows that Bering Sea assemblages are transitional from those from the shelf regions of the Arctic Ocean proper. Results indicate that the Bering Sea samples differ from the Arctic samples in having larger proportions of *N. leioderma* and *S. bradii* and much lower proportions of *P. pseudopunctillata*. There were no sharp boundaries among the sample groups, which probably reflects salinity and temperature regimes that are discussed below.

Ocean Temperature

The ocean temperature regimes of the Bering and Chukchi Seas appear to strongly influence the composition of ostracode assemblages living in each region, which are dominated by species adapted to Arctic and subarctic climates. Mean September and January sea-surface temperatures (SST) near St. Lawrence Island are about 5-7°C in September and -1.7°C (the

approximate freezing point of seawater) in January (Figure 1.3). Summer bottom water temperatures in the Bering Sea range from about 0.7°C to almost 4°C since 1982, and even warmer along the coast due to the influence of Alaskan Coastal water. In the central Chukchi Sea, mean September and January SSTs are 1-2°C and -1.7°C, respectively, and are mostly sea-ice covered. Near shore, September temperatures can reach 2-4°C and higher in coastal estuaries.

The temperature sensitivity of ostracode species is illustrated by the geographic distributions of two species within the Bering Sea (Figure 1.6). The circum-Arctic species *P. pseudopunctillata* is common (25-30%) only in the northern most Bering Sea near the Bering Strait (63-64°N latitude). In contrast, the temperate species *Pectocythere janae* is primarily distributed near latitude 62°N, south of St. Lawrence Island where it was found mainly during relatively warm years in the early 2000s. Its presence in the central Bering Sea reflects its northernmost geographic range limit, with the important exceptions of its occurrence in very low numbers along shallow margins of the East Siberian and Beaufort Seas in sediments only collected in 1979-1980. In the Chukchi Sea samples studied here, *P. janae* comprised 7.8% of the total assemblage in 2009, and 5.1% in 2010. These occurrences may represent a recent range extension from the southwest Bering Sea through the Bering Strait, but additional samples are needed to confirm this species has established itself in the Chukchi. In summary, based on all available data,

P. janae inhabits the Bering Sea and the margins of the western Arctic Ocean only periodically in waters with temperatures exceeding about 0-2°C.

In contrast to the Bering Sea, the dominance of circum-Arctic cryophilic species, such as *P. pseudopunctillata* in the Chukchi Sea, reflects an assemblage suited to live at annual temperatures remaining $\sim +2^{\circ}\text{C}$, except along coastal margins. *P. pseudopunctillata* also dominates the Laptev Sea assemblages, sometimes representing up to 80% of the total assemblage.

S. bradii is another species adapted to cold temperatures (Figure 1.7).

Samples from relatively cold years of 1994 and 1999 (Figure 1.7A) and 2009 and 2010 (Figure 1.7C) contained abundant *S. bradii*, sometimes reaching 50-80% of the assemblage. In contrast, samples from warmer years of 2001-2006 (Figure 1.7B) show its abundance declined to <10% of assemblage in almost all samples.

Spatial and temporal patterns in Bering and Chukchi ostracode assemblage variability are challenging to interpret because of large changes in temperature and sea ice during the past few decades. For example, the northern Bering Sea shelf has experienced significant sea surface warming, particularly in fall and summer, since 1982 (Brown et al., 2011). Similarly, there is considerable evidence for changes in Pacific Water influx and heat transport through the Bering Strait (Woodgate et al., 2010), Atlantic Water

temperature variability in the Western Arctic Basin (Polyakov et al., 2011), and increasing Chukchi Sea temperature (Belkin, 2009) during the past few decades. Moreover, climate model simulations predict continued warming in both the North Pacific and Arctic. According to Wang et al. (2012), air temperature increases will be most significant in late fall (November to December) for both the Chukchi and Bering Seas, with increases by 2050 of 3°C for the Bering Sea and increases in excess of 5°C for the Chukchi Sea. Consequently, continued changes in air and ocean temperature, sea-ice extent and duration can be expected to continue to alter Bering and Chukchi ostracode assemblages and other aspects of the ecosystem structure and function.

Salinity

In the Arctic Ocean, ostracode assemblages along the coastal margins of the Kara and Laptev Seas show the strong influence of salinity, which varied from < 5 to > 32 due to freshwater influx near the mouths of the Ob', Yenisei and Lena Rivers (Stepanova et al., 2007). Brouwers (1988a) also found that salinity influenced ostracode assemblages in Gulf of the Alaska. In the central Bering Sea, salinity variability is relatively small (31-33) compared to that in coastal zones such as Norton Sound area, where salinities can range as low as 22-28 due to freshwater discharge from the Yukon River (Figure 1.8).

Cytheromorpha macchesneyi and *P. pseudopunctillata* were common in some samples from the Norton Sound area in the eastern part of the study region (Figures 1.9A and 1.9B). Both species are known to tolerate low and fluctuating salinities near and in Arctic estuaries, fjords and other runoff-influenced coastal zones. The influence of lower salinity in coastal zones was also reflected in the distribution of *C. macchesneyi* and *P. pseudopunctillata*, which is shown in cross section from the Beaufort Shelf to the Bering Sea-Norton Sound area (Figure 1.10). These species are only found in shallow water, near coastal regions because they tolerate lower salinities. Their distributions best coincide with coastal waters associated with the Alaska Coastal Current. In contrast, *P. janae* and *S. complanata*, two stenohaline species, were more common where salinity is relatively constant, further to the west and south of St. Lawrence Island (Figure 1.9A and 1.9B).

Productivity

Herman et al. (1999) showed a dependence of benthic biomass on the magnitude of the spring phytoplankton bloom in many shallow, well-mixed estuarine systems such as Chesapeake Bay, San Francisco Bay, Bay of Fundy, Columbia River estuary, and Ems estuary (Wadden Sea). However, very few studies of shallow water marine ostracodes have examined the possible relationship between primary productivity and ostracode species.

Steineck et al. (1985) and Yasuhara et al. (2009) are exceptions and noted that some benthic ostracode species are influenced by surface productivity. I found that the abundance of the cryophilic species *N. leioderma* declined with increasing SSTs and decreasing productivity, whereas abundance of *P. janae* increased with warmer SSTs and higher productivity (Figures 1.11A and 1.11B).

A possible relationship between these species and productivity is apparent in plots of percent abundance of *N. leioderma* (Figure 1.12A) and *P. janae* (12B) against satellite based estimates of primary productivity that were estimated for the Inner Shelf, along the eastern Bering Sea by Brown et al. (2011).

Since these satellite observations of surface productivity do not penetrate to subsurface chlorophyll, and are dependent upon color algorithms, these productivity trends may be underestimated or otherwise incorrect. However, if I assume that this data are generally representative of the broad shelf ecosystem, *N. leioderma* was most abundant during times of reduced productivity ($r^2=0.49$). This is consistent with the known ecology of *N. leioderma* as a eurytopic species. In contrast, *P. janae* appeared to be more abundant during those years when productivity was higher ($r^2=0.63$), consistent with its stenotopic specialization. For the other Bering Sea ostracode species analyzed, no apparent relationship was found between abundance and primary productivity, at least for the periods 1998-2010. Direct measurements of productivity coupled with additional assemblage data

would improve our understanding of species-productivity relationships.

Primary Productivity and Species Diversity

Another aspect of the Bering Sea ecosystem addressed here is the question of what factors control species diversity in Arctic and subarctic ostracodes. Despite representing a smaller collection in samples and temporal coverage, the Chukchi ostracode assemblage had higher species diversity than did the Bering Sea (28 versus 21 species). This is mainly because Chukchi assemblages included small but significant numbers (~2-10%) of several cryophilic circum-Arctic species (*Elofsonella concinna*, *Finmarchinella angulata*, *Cluthia cluthae*, *Roundstonia globulifera*, and several species of *Cytheropteron*). The difference in species diversity in the Bering and Chukchi assemblages could be due to several factors. The continental shelf is a highly variable environment, and ostracode diversity is often low in regions where significant physical and chemical changes occur rapidly and/or frequently (Boomer and Eisenhauer, 2002). According to Yasuhara et al. (in press), Arctic ostracode diversity is strongly affected by surface productivity, and seasonality of productivity in shallow Arctic marine environments. Therefore, productivity, in particular the timing, amount and length of primary production, may affect the benthos of the Bering and Chukchi shelves. Surface primary production on the Bering shelf averages 120-150 g C m⁻² yr⁻¹

and comes in a short pulse in May through July (Brown et al., 2011). Other older estimates of Northern Bering Sea production range even higher from 250-470 g C m⁻² yr⁻¹ (Springer and McRoy, 1993; Springer et al., 1996). While Brown et al. (2011) also found that net primary production exhibited no clear long-term trend during the past several decades; annual production varied by year depending the duration of the ice season. Lee et al. (2011) have reported a recent decline in Bering Sea primary production in 2007 compared with the 1980s. The Chirikov Basin is the only area within the Bering Sea that is experiencing an increase in ice-free days, which may allow a longer productivity window. Sea-ice extent throughout the rest of the Bering shelf is not in decline. While there is a clear connection between sea ice break-up and primary production in the spring, the influence of earlier sea-ice retreat in the northern Bering Sea upon water column productivity is difficult to anticipate due to interconnected complexities such as water column mixing from winds (Cooper et al., 2012).

In contrast, the Chukchi Sea spring sea-ice retreat over the past several decades, has been consistently earlier and fall sea-ice formation consistently later, which produces a longer season to support primary productivity (Arrigo et al., 2011). Mean annual primary productivity in the southern Chukchi Sea ranged from 80-840 g C m⁻² yr⁻¹ in certain “hot-spot regions” in the 1990s (Springer and McRoy, 1993; Springer et al., 1996). Generalized satellite observations of primary production indicated a 48% increase over a 12-year

period from 1998 to 2009 (Frey et al., 2011).

Therefore, with the open water season available to support primary productivity lengthening in the Chukchi, it is reasonable to assume that additional organic carbon is reaching the seafloor and it may influence the benthic community, including ostracodes. The species-energy hypothesis suggests that biodiversity is positively correlated with productivity because more productive ecosystems can sustain more individuals (Gaston, 2000). If the Bering Sea's primary productivity is declining, it may in part explain the lower ostracode species diversity observed in the Bering. Increasing productivity may be one explanation for the Chukchi Sea's greater ostracode species diversity. However, the underlying mechanisms impacting ostracode diversity are complex, and ecological preferences of individual taxa and oceanographic characteristics of a particular region all likely play a role. Furthermore, this analysis is cursory because a far greater number of Bering Sea samples (225) were analyzed compared to the Chukchi samples (16).

Summary

As an initial effort to examine the effects of recent climate and oceanographic changes in the northern Bering and Chukchi Seas on ostracode assemblages, the results presented here lead to several preliminary

conclusions. First, the spatial distributions of ostracode species in the Bering-Chukchi region appear to be controlled by ocean temperature, and to a lesser extent salinity (in Norton Sound) and productivity (for selected species such as *P. janae*). Second, decadal changes in the benthic meiofauna in the Bering Sea during the past 35 years were most likely caused by ocean temperature, sea-ice cover and related ecosystem changes. Results presented here also provide baseline data on species distributions and diversity that can be used in future studies assessing Arctic and subarctic ecosystems and their response to climate change. The following chapter, Chapter 2, will expand the discussion of temperature as the primary factor controlling Bering Sea ostracode abundance and geographic distribution by exploring the changes in dominant species' abundance together with consideration of ecology of key taxa.

Figures 1.1 – 1.12

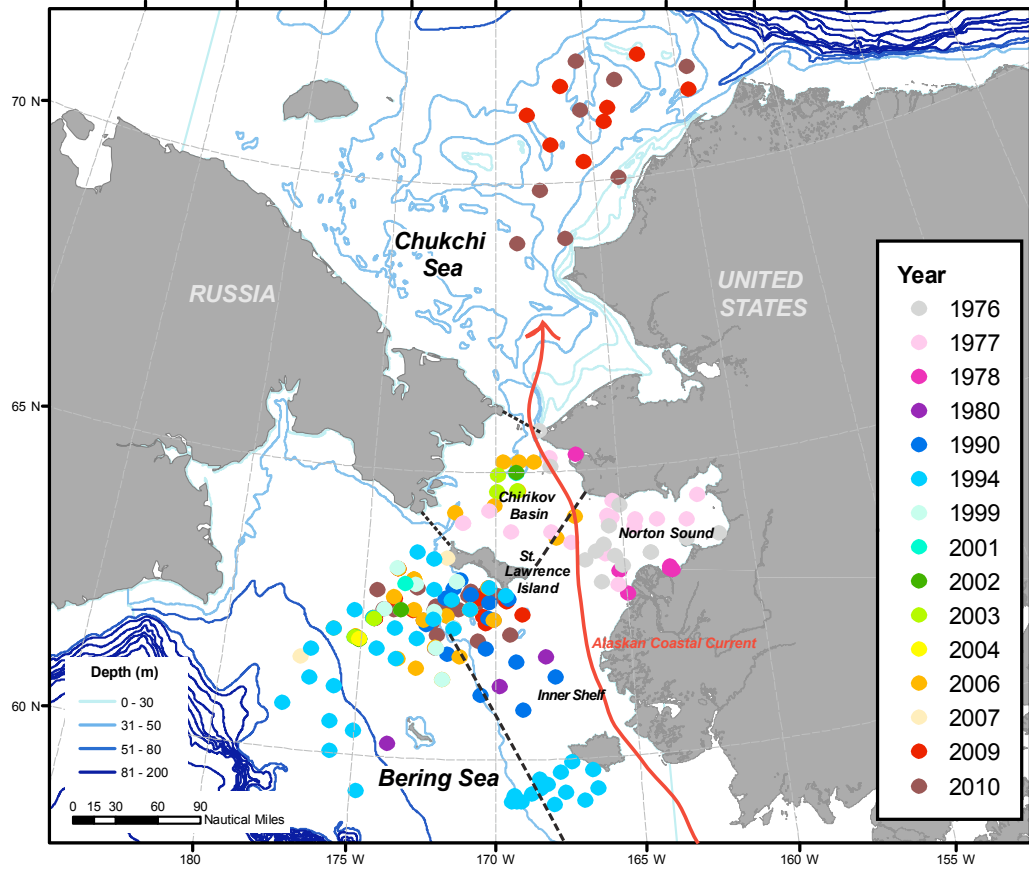
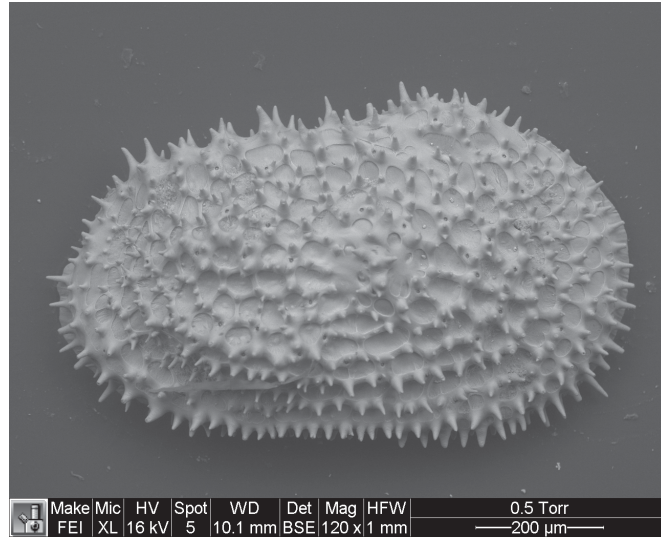


Figure 1.1. Location of sediment samples used in the present study of benthic ostracodes and areas discussed in the text by year: Chukchi Sea, Bering Sea, Norton Sound, Chirikov Basin, Inner Shelf region off western Alaska, Alaskan Coastal Current.

A



B

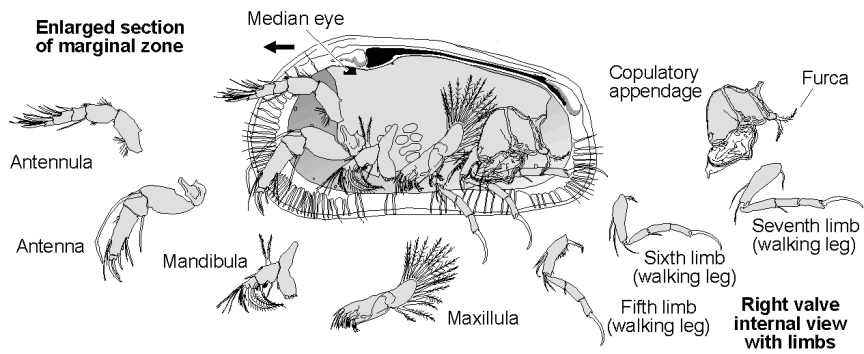
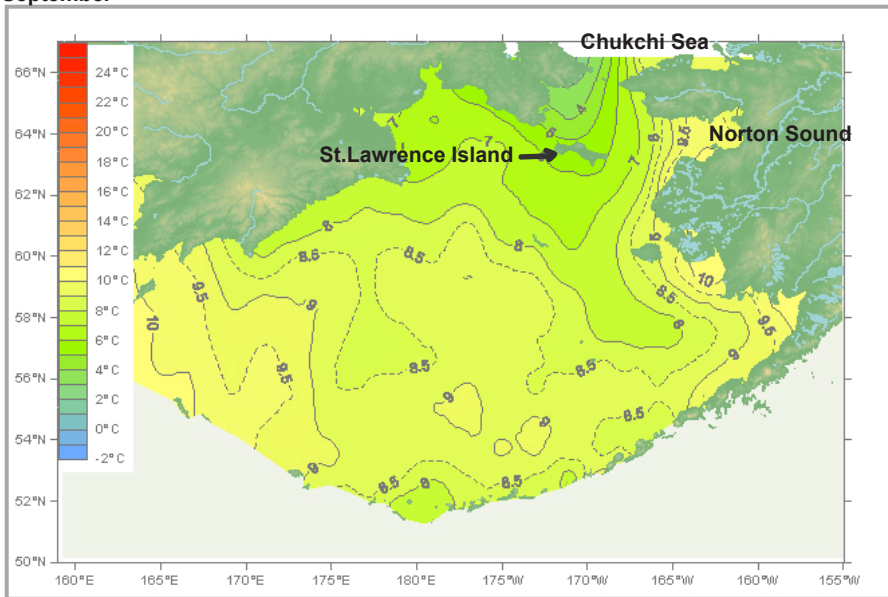


Figure 1.2. Scanning electron photo of Arctic ostracode *Henryhowella cf. asperrima*, adult female, right valve (1.2A) and general anatomy of a Podocopid ostracode (1.2B). [Photo courtesy of Moriaki Yasuhara and illustration courtesy of David Horne as published in Horne et al., (2002)]

A. September



B. January

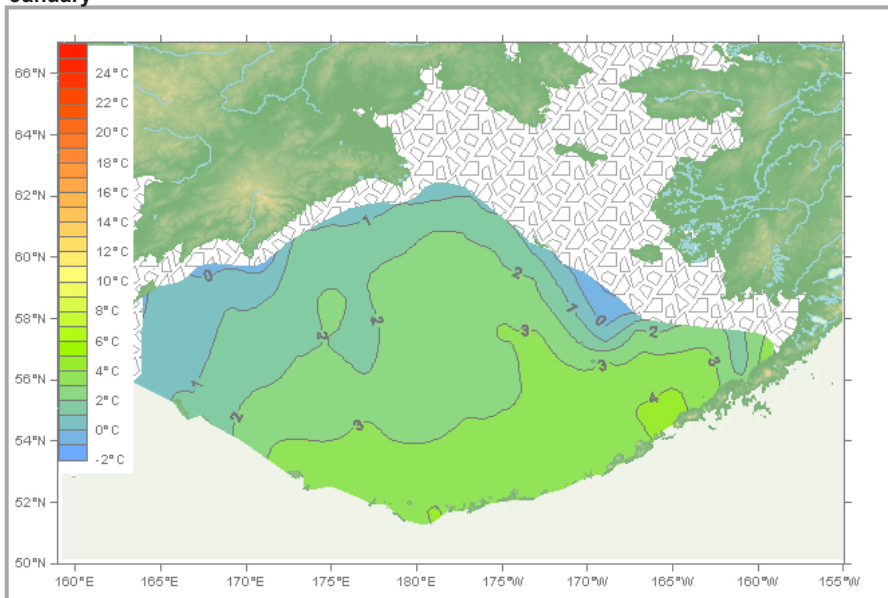


Figure 1.3. September (1.3A) and January (1.3B) sea-surface temperatures (SST) representing mean summer and winter temperatures, respectively. Maps are web-based products from the U. S. National Oceanic and Atmospheric Administration National Oceanographic Data Center (NODC): <http://www.nodc.noaa.gov/cgi-bin/OC5/PACIFIC2009/showclimatmap.pl>

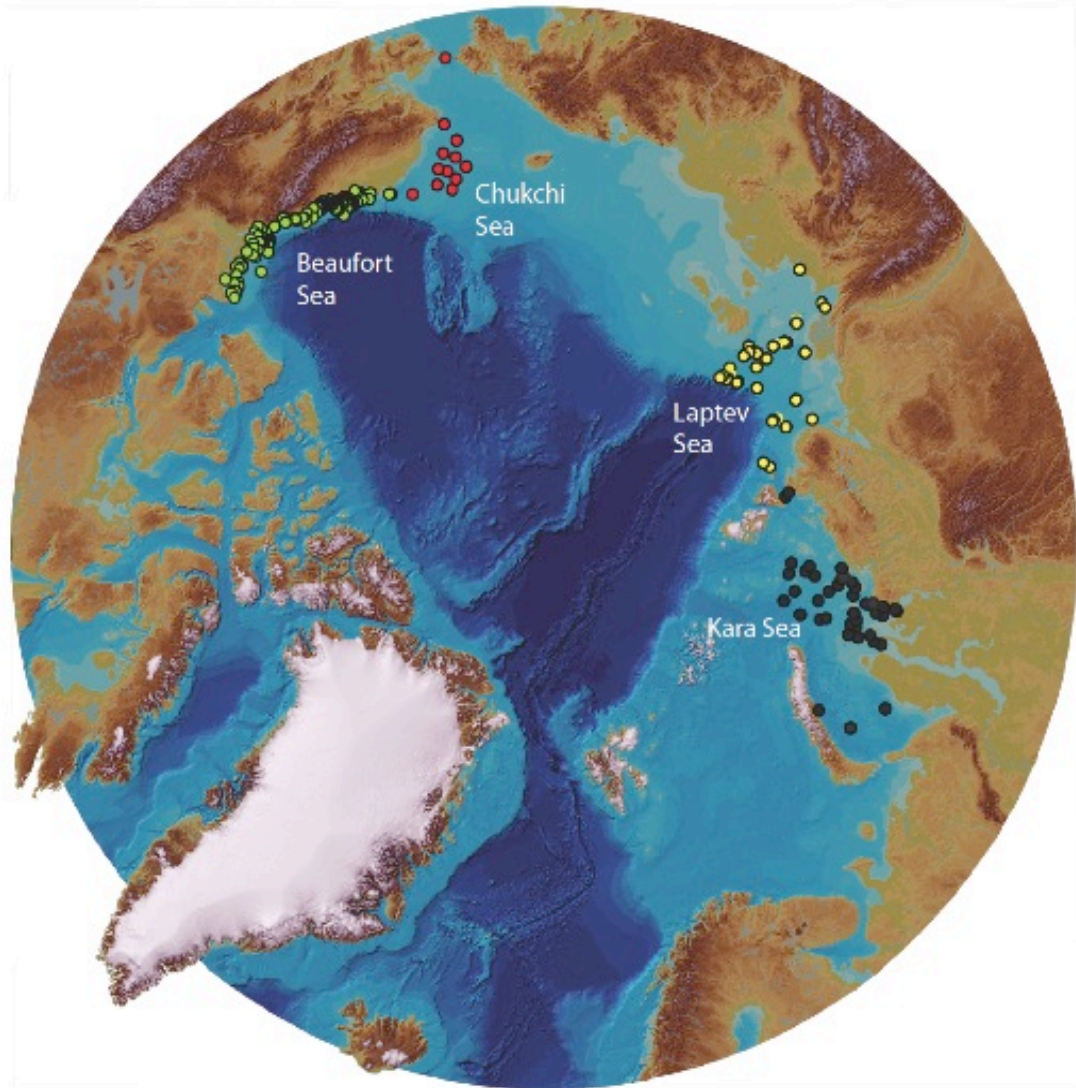


Figure 1.4. Map showing locations of circum-Arctic continental shelf ostracode samples used in comparative biogeographic analysis of Bering and Chukchi Sea ostracode assemblages.

Map derived from: <http://www.ngdc.noaa.gov/mgg/bathymetry/arctic/currentmap.html>

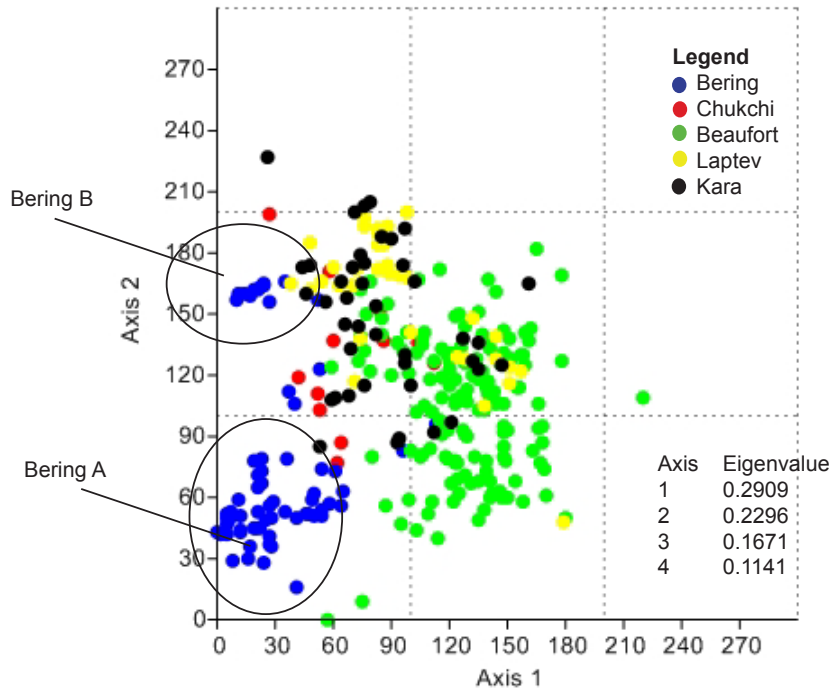


Figure 1.5. Detrended correspondence analysis (DCA) comparing Bering and ostracode assemblages with those from circum-Arctic shelves shown in Figure 1.4 (n=306, 43,200 specimens). This representation illustrates how ostracode assemblages in near-shore marine Arctic environments differ from northern Bering Sea assemblages. Colored circles represent sample locations: Bering (blue dots), Chukchi (red dots), Beaufort (green dots), Laptev (yellow dots), and Kara (black dots). “Bering A” sample group plots low on axis two and includes larger proportions of *N. leioderma* and *S. bradii*, while “Bering B” group contains larger proportions of *S. complanata* represented in 2006 and 2009 samples. There are no sharp boundaries among the samples; the gradations between the samples are due to differences in years collected and the geographically varied salinity and temperature regimes of the regions. (Samples with <20 specimens and samples with from water depths ≥ 200 m were excluded.)

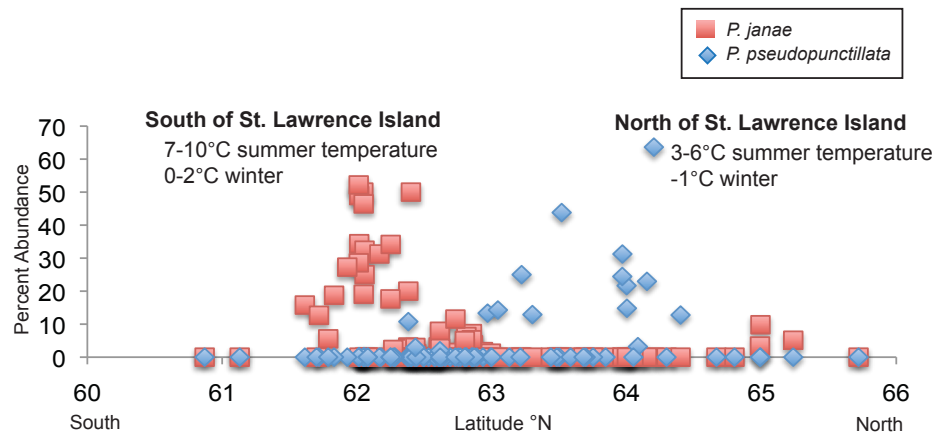


Figure 1.6. Percent abundance and latitudinal distribution of circum-Arctic species *P. pseudopunctillata* and temperate species *P. janae* in the Bering Sea. *P. pseudopunctillata* is common only in the northern most Bering Sea near the Bering Strait (63-64°N latitude), where it likely migrates from the Beaufort Sea region. In contrast, the temperate species *P. janae* is primarily distributed near latitude 62°N, south of St. Lawrence Island where it presumably migrates north from the Gulf of Alaska during periods of warmth in the Bering Sea.

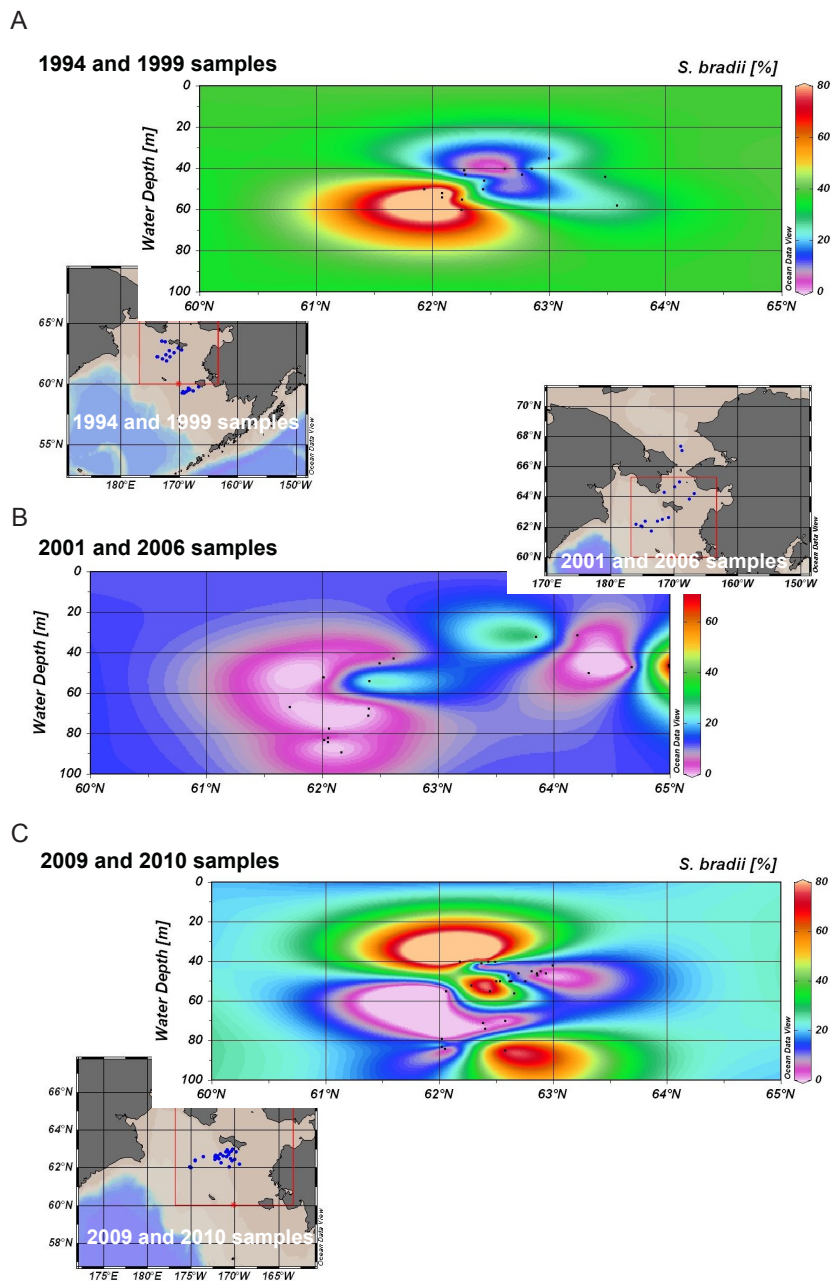


Figure 1.7. Abundance of *S. bradii* during three intervals showing the principal temperature control of its abundance. Samples are denoted by the blue dots on the respective maps, from relatively cold years of 1994 and 1999 (1.7A) and 2009 and 2010 (1.7C) show its abundance increases to sometimes 50-80% of the assemblage. In contrast, samples from the warm years of 2001-2006 (1.7B) show its abundance declines to <10% of assemblage in all but two samples.

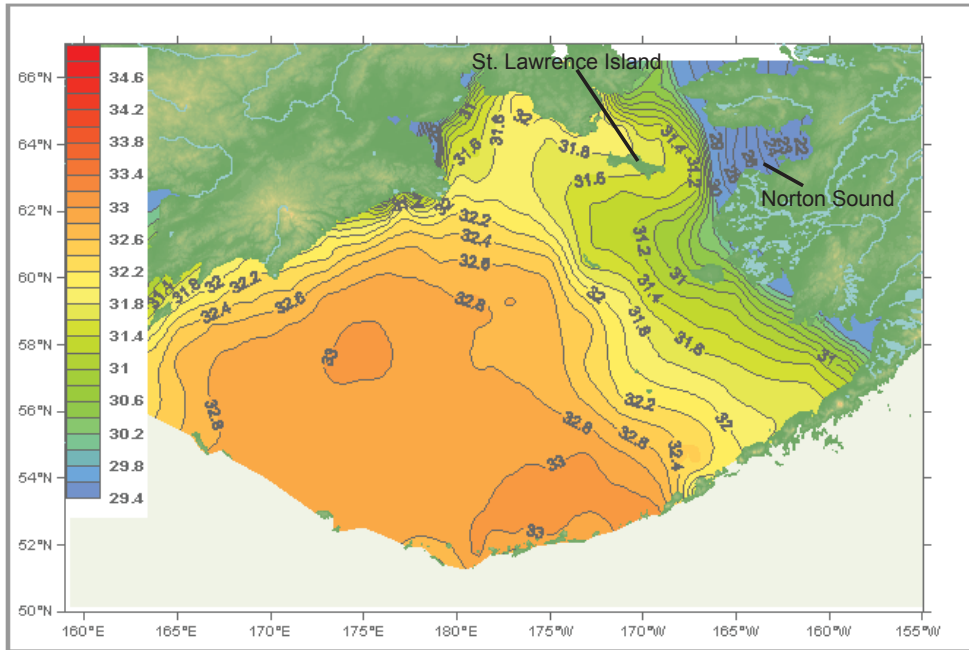


Figure 1.8. Salinity in the Bering Sea and Norton Sound region in September 2009.
Map derived from:
<http://www.nodc.noaa.gov/cgibin/OC5/PACIFIC2009/showclimatmap.pl>

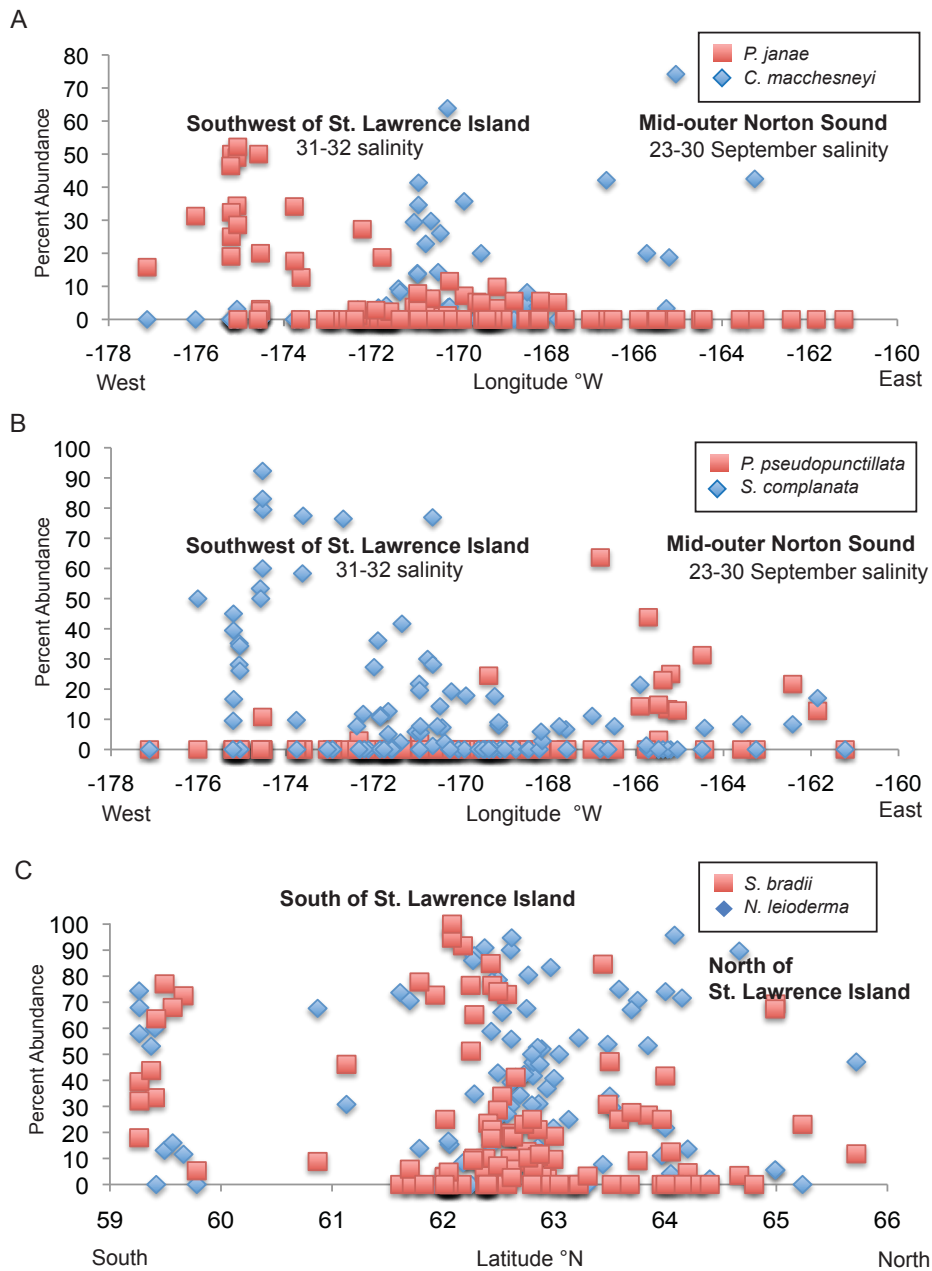


Figure 1.9. Longitudinal distribution of *P. janae* and *C. macchesneyi* in the Bering Sea (1.9A), showing *P. janae* is most abundant in the southwestern part of the study region, while *C. macchesneyi* is abundant in the central and eastern (Norton Sound) regions. Longitudinal distribution of *S. complanata* (southwest region) and *P. pseudopunctillata* (Norton Sound) (1.9B). The latitudinal distribution of *S. bradii* and *N. leioderma*, the two most common species in the northern Bering Sea, shows that occur together and this reflects their eurytopic ecology (1.9C). Plots are based on 110 samples collected between 1976-2010 and having >10 total specimens in each sample.

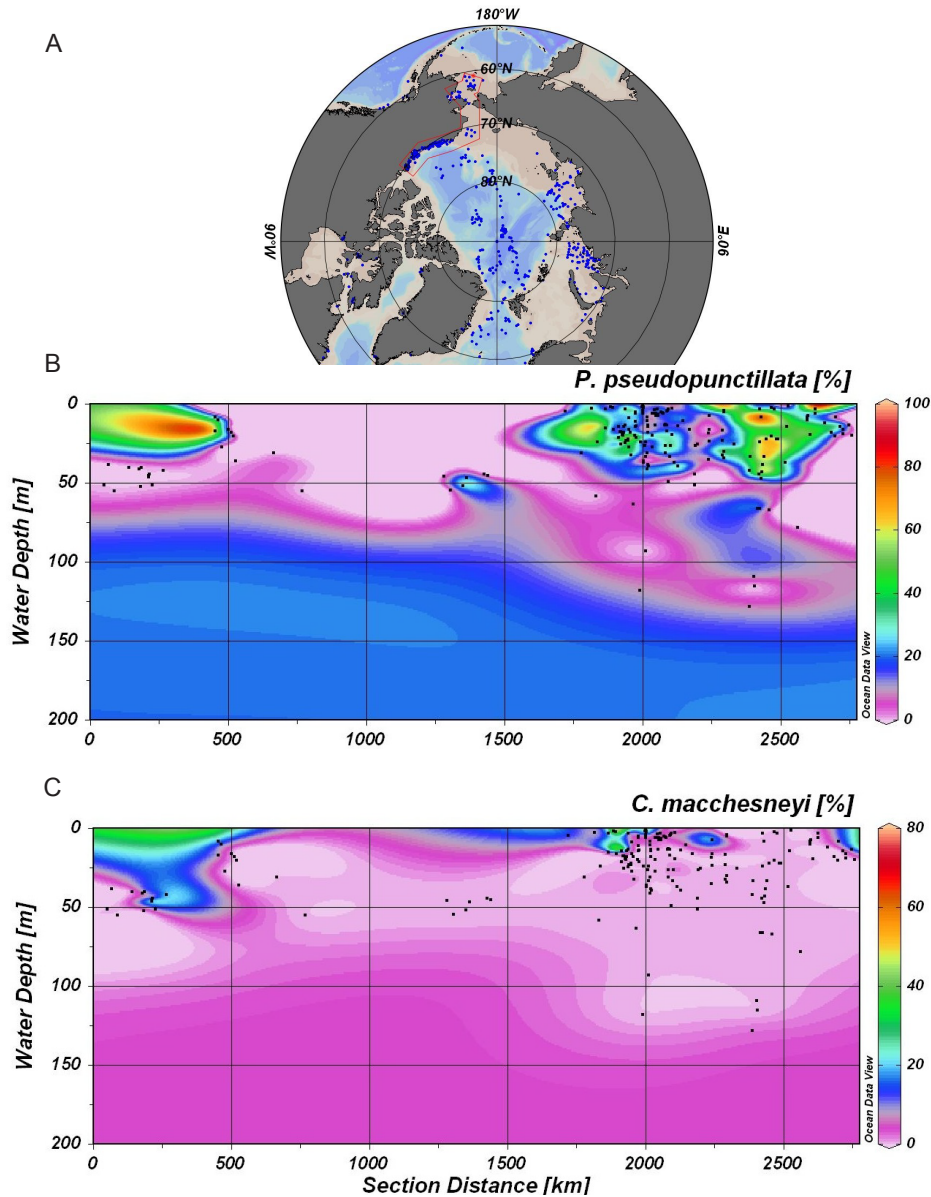


Figure 1.10. Contour plots of distribution, depth and abundance of *P. pseudopunctillata* (1.10B) and *C. macchesneyi* (1.10C) along a transect of the northern Bering/Chukchi/Beaufort Sea (outlined in red) (1.10A, map). Transect runs from the northern Bering to Chukchi and then into the Beaufort Sea. Blue dots on map show a 700-surface-sample ostracode database combined with Bering Sea samples from the current study (Figure 1.1). The distributions of *C. macchesneyi* and *P. pseudopunctillata* appear to be influenced by the Alaska Coastal Current, which flows along the western Alaskan coast into the Chukchi and Beaufort Seas. The abundance *P. pseudopunctillata* is a dominant species along the coasts of the Chukchi-Beaufort Sea representing on average 40-80% of the assemblage. *C. macchesneyi* is common (>30% of assemblage on average) along the Chukchi-Beaufort shallow margins.

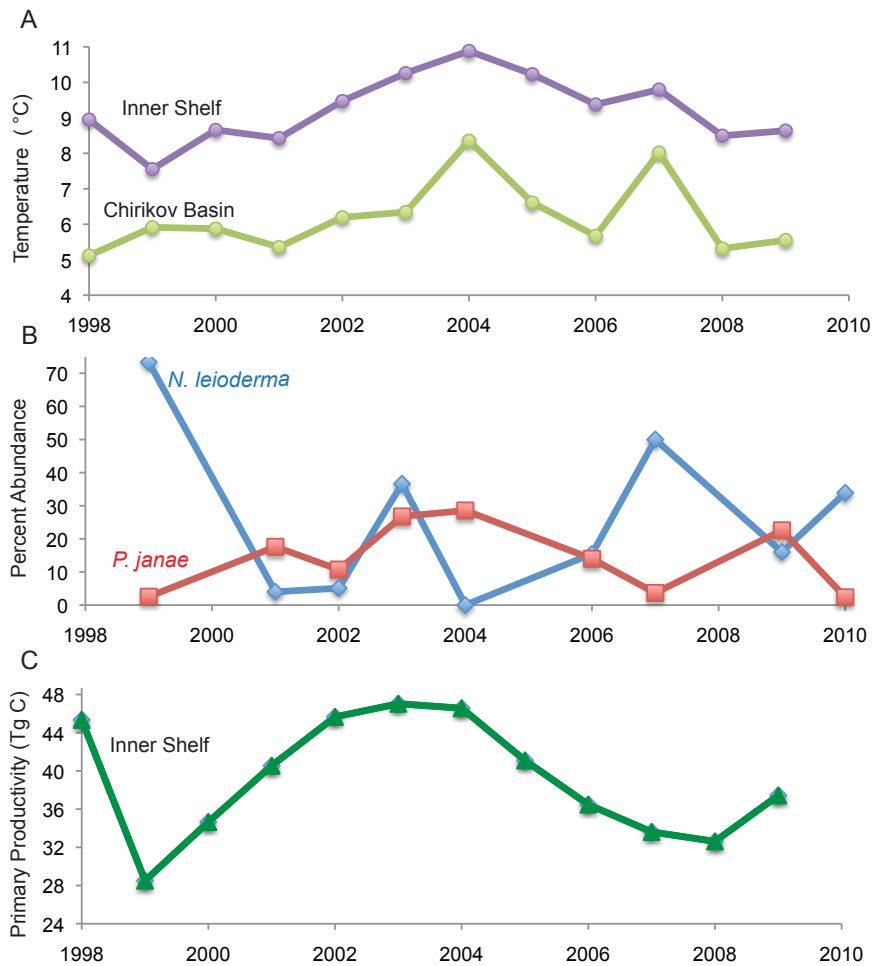


Figure 1.11. Summer sea-surface temperature (SST) from the Chirikov Basin and Inner Shelf regions (1.11A) plotted against percent abundance of *P. janae* and *N. leioderma* since 1998 (1.11B). Primary productivity in the Inner Shelf (1.11C) is plotted from 1988 to 2009. (SST and primary productivity data courtesy of Zach Brown as presented in Brown et al., 2011. I define the Inner shelf region (<50 m depth) to include the Eastern Bering shelf and the Gulf of Anadyr (bounded by Cape Navarin to the south, St. Lawrence Island to the east, and Cape Chukotskiy to the north.)

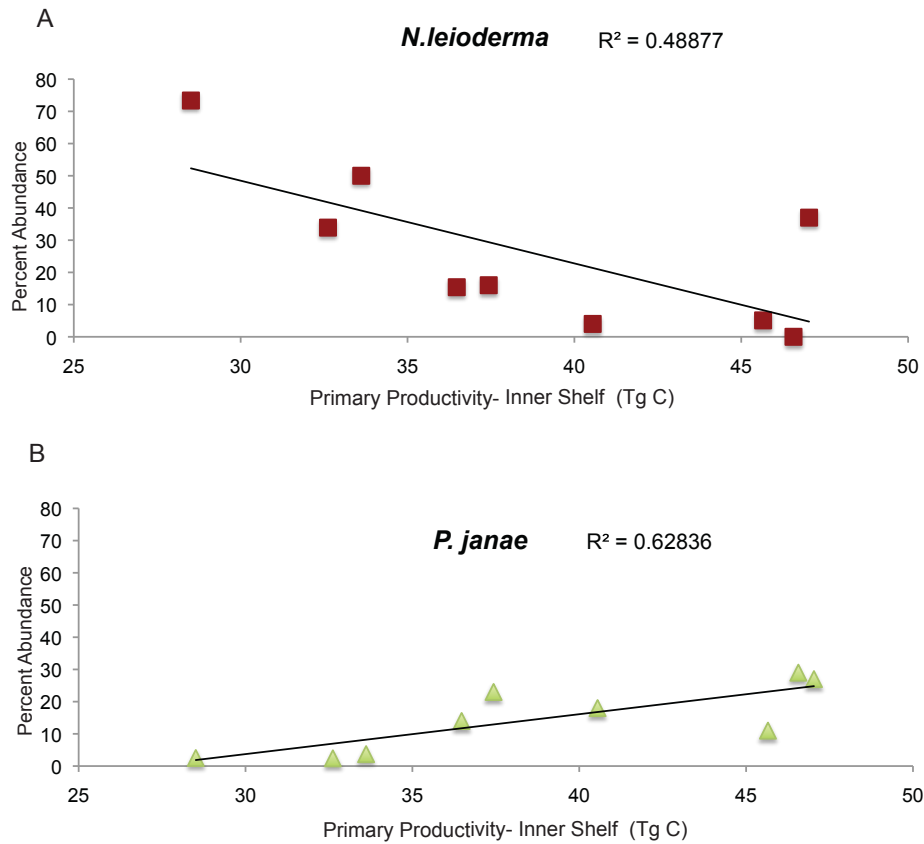


Figure 1.12. Percent abundance of *N. leioderma* (1.12A) and *P. janae* (1.12B) plotted as a least-squares fit regression against primary productivity as measured in the Inner shelf of the eastern Bering Sea. *N. leioderma* is significantly more abundant as productivity is reduced ($r^2=0.49$). In contrast, *P. janae* abundance is correlated with higher productivity ($r^2=0.63$).

Chapter 2: Temporal Changes in Benthic Ostracode Assemblages in the Northern Bering and Chukchi Seas from 1976 to 2010

Introduction

As surface temperatures rise in the Arctic Ocean and sub-polar seas, satellite observations document a corresponding reduction in the extent, thickness, and duration of seasonal sea-ice cover (Stroeve et al., 2008). In recent years, Arctic multi-year ice has declined by almost 50% in extent, and fall freeze-up occurs later in the year (Serreze et al., 2007; Stroeve et al., 2008). Model results indicate these trends will continue, and that the Arctic Ocean might become predominantly ice-free in summer in a few decades (Wang and Overland, 2009). These sea-ice retreats have been particularly dramatic in the Arctic Ocean just north of the Bering Strait; sea-ice retreats in 2007 and 2009 lengthened the open-water season by about four weeks (Grebmeier et al., 2010).

While these patterns of sea-ice decline are well documented, much less is known about the responses of biological communities to ice cover changes. Here I present new data on benthic ostracode distributions from the Chukchi

continental shelf, the Chirikov Basin of the northern Bering Sea, and the area south of St. Lawrence Island (Figure 2.1). Ostracodes are environmentally sensitive, and water temperature is one of the most influential factors controlling species' reproduction, survival and geographic distributions (Hutchins, 1947; Smith and Horne, 2002). I sought to determine whether the recent changes in temperature and ice cover have affected species distributions. To the best of my knowledge, this is the first published report on modern ostracode fauna from the northern Bering shelf. Adjacent areas where ostracode data are available include the Chukchi/Beaufort Seas (Joy and Clark, 1977) and the Gulf of Alaska (Brouwers, 1990; 1993; 1994).

Environmental Setting

The Bering and Chukchi Seas are among the world's most seasonally productive ecosystems, supporting high, seasonal primary productivity that exceeds $1 \text{ g C m}^{-2} \text{ d}^{-1}$ during the spring bloom (Brown et al., 2011), diverse invertebrate, fish, seabird, and marine mammal populations (National Research Council, 1996). Two-thirds of the Bering Sea is made up of an 800-km wide continental shelf to the north and east, which ranges in depth from 10-50 meters deep (Figure 2.1). This shelf continues through the Bering Strait and becomes the Chukchi continental shelf in the western Arctic Ocean.

The Bering Sea is located in a transition region between a generally cold, dry Arctic air mass to the north and moist, relatively warm air to the south (Mantua and Hare, 2002). Hunt and Stabeno (2002) concluded that southeastern Bering Sea climate is jointly influenced by both the Pacific Decadal Oscillation (PDO) and the Arctic Oscillation (AO). The PDO is a multi-decadal pattern of Pacific climate variability involving air-ocean interactions that create current and sea surface temperature changes in the North Pacific (Mantua and Hare, 2002). In contrast, the northern Bering Sea, which I define as the shelf north of St. Matthew Island, and the Chukchi Sea are more directly influenced by the AO (Grebmeier et al., 2006a; 2006b). The state of the AO is determined by the atmospheric pressure gradient in the high Arctic, and it alternates between negative (high pressure over the North Pole) and positive (low pressure) modes. This coupled air-sea interaction is closely linked to the strength and position of the Beaufort Gyre in the Arctic Ocean. From 1989 to 2006, the AO was predominantly in a positive mode, causing lower Arctic air pressure and higher sea-to-air temperatures in the Arctic (Overland et al., 2008). NOAA's Climate Prediction Center (<http://www.cpc.ncep.noaa.gov/>) indicates that the AO has been in a negative mode the past two years but has exhibited an overall positive trend since 1990.

These air-sea interactions and, possibly also anthropogenic factors, have contributed to interannual and decadal changes in temperature and sea ice in

the North American Arctic over the last several decades (Overland et al., 2008; Serreze et al., 2007). Circulation in the Bering and Chukchi Seas is influenced by three northward flowing water masses arrayed east to west: less saline Alaska coastal water; a mixed, more saline water mass to the west; and a seasonally cold and even more saline Anadyr water mass further to the west (Stabeno et al., 2007; Belkin et al., 2009). As these water masses extend into the Chukchi Sea, the differences between the mixed shelf water and Anadyr water become less distinct; there are also differences in temperature and salinity depending upon when the water passes through Bering Strait.

One example of ongoing change being observed is that the Chirikov Basin gained ~25 annual days of open water during the past 25 years (Figure 2.2). This has changed not only the timing of when primary productivity peaks but may also increase production due to a longer, sustained bloom (Brown et al., 2011; Arrigo et al., 2008). It is expected that continued warming and sea-ice change will impact biological communities with cascading consequences through the food web (Grebmeier et al., 2012; Mueter and Litzow, 2008).

Despite these expected and observed changes in the northern Bering Sea and Chukchi Sea, it is important to note that similar sea-ice changes are not being consistently observed further to the south. In winter, the southern margin of sea-ice coverage in the Bering Sea reaches an annual maximum by

March, but sea ice is in part uncoupled from sea-ice retreat to the north because of the semi-enclosed nature of the marginal sea. Ice duration in the southern Bering Sea and along the Inner Shelf, although varying from year to year, has not consistently changed over the time period (1976-2010) I consider here (Figure 2.2; Brown et al., 2011). (The Inner shelf region is defined to include the Eastern Bering shelf adjacent to Alaska and the Gulf of Anadyr, bounded by Cape Navarin to the south, St. Lawrence Island to the east, and Cape Chukotskiy to the north.)

Materials and Methods

Ostracode Sampling

A total of 225 northern Bering Sea surface sediment samples containing 5972 ostracode valves and carapaces were collected during a number of cruises from 1976-2010 (Table 2.1). Most samples came from the central and northern Bering Sea continental shelf, with additional samples also from Norton Sound in 1976-78 (Figure 1.1). The 1977 cruise also included sampling locations in the Chirikov Basin. Sixteen surface sediment samples from the Chukchi shelf contained 1198 specimens. Samples were from water depths ranging from 10 to 110m and were taken from the top of Van Veen grabs before the grab was opened, or from the top of HAPS and box corers.

Sediments ranged from muddy or silty clay to sandy. Ostracodes were generally more abundant in silty clay sediments than in coarser sandy sediments, which likely results from lower deposition in more hydrodynamically active areas.

Ostracode assemblages preserved in continental shelf surface sediments can typically represent the fauna living at or near the time of collection (with a few exceptions, this study involved spring and summer cruise collections).

Sometimes the shells of molts or dead specimens from prior years are also recovered. In the case of Bering Sea ostracodes, most assemblages included adult specimens and juvenile molts, and 60% of the specimens were articulated carapaces, or carapaces with chitinous appendages. A few samples contained Rose Bengal-stained specimens, a stain that is absorbed by cell cytoplasm to help distinguish specimens that were alive at or near the time of collection. Because the stain highlights physical structures, specimens can be viewed more clearly under microscopic magnification. Some reworked specimens from prior years, identified by broken or abraded specimens, are to be expected in a continental shelf setting; however, in our samples, reworked specimens were relatively rare. Thus, I consider the faunal data presented here to be representative of the time of collection and useful for detecting decadal and, in some cases, large interannual changes in the ecosystem.

Sample Processing

Ostracodes were separated from 20 to 100 g sediment aliquots by washing the samples with tap water through a 63 μm sieve. Samples were then dried in a convection oven at 50°C for 12 to 24 hours. The >63 μm size fraction includes adults and most juvenile molts of all species. Ostracodes were removed from the >125 μm sediment size fractions with a fine, damp brush under a light microscope and placed on a slide. Because early instars can be the same size as sand grains, it is typical that the >125 μm size fraction is used for analysis (Cronin et al., 2011). Species were identified primarily following the taxonomy and scanning electron microscope (SEM) imagery provided in Stepanova et al. (2007 and 2010) and Brouwers (1990, 1993, 1994). Identification is based primarily on physical features such as carapace morphology (shape and size), pore size, and pore distribution, hinge characteristics, and shell ornamentation.

The relative abundance (or relative frequency) of each species was expressed as a percentage of the total assemblage. Percentage abundances were computed by dividing the number of individual species found in each sample by the total number of specimens found in that sample and then multiplying the result by 100 to convert to percent. Relative abundance is a valid measurement to detect differences in populations and is considered the standard convention in micropaleontology (Buzas, 1990; Imbrie and Kipp,

1971). An assumption of this method is that changes in ostracode species abundance are attributable to physical and chemical changes in the environment, as these factors have the greatest large-scale control on species. Density was calculated by dividing the total number of ostracode specimens found in each sample by the dry sediment weight (grams) of that sample. However, abundance per dry gram is highly variable depending on many factors, such as sediment grain type, time of year and individual species environmental preferences

Sources of Temperature and Sea-ice Data

Mean summer Sea Surface Temperature (SST) data (1982–2009) for the Chirikov Basin and Inner Shelf regions are based on satellite data from the Reynolds Optimum Interpolation SST (OISST) Version 2 product, which is derived from the Advanced Very High Resolution Radiometer (AVHRR) platform at 0.25° resolution. “Summer” is defined as July, August and September. Annual mean Bering Sea summer bottom water temperatures (BWT) and May SST (Figure 2.5A) were obtained from the Bering Climate and Ecosystem data archive (<http://www.beringclimate.noaa.gov/data/>). BWT data were collected from bottom trawl surveys across the eastern Bering Sea shelf from early June to early August, during the years 1982–2007. The spatial coverage spans approximately 54.5–62°N and 179–158°W, with

stations gridded at roughly 20 nautical miles distance (248–317 stations/yr).

The May SST data used were collected in the southeastern Bering Sea (54.3-60.0°N, 161.2-172.5°W), which is probably the best long-term regional water temperature data set that is available. These data are summarized from the NCEP/NCAR Reanalysis project (Kalnay et al., 1996). Index values of the data are defined as deviations from the mean value (2.48°C) for the 1961-2000 period normalized by the standard deviation (0.73°C). The northern and southern Bering have different temperature histories, with more recent seasonality in the north due to greater surface warming from the influence of Alaska Coastal water. Although this southeastern Bering record does not precisely reflect the temperatures at our study area, it is the best available annual spring-summer record and represents regional temperature patterns for the last few decades.

Statistical Analyses

All statistical tests were performed with PAST (PAleontological Statistics; Hammer et al., 2001) PAST is a comprehensive statistics package that runs a range of standard numerical analysis and operations used in quantitative paleontology and many fields of earth science. Several multivariate techniques (cluster, detrended correspondence and canonical correspondence analyses) were used to provide a consistent way to search

for patterns in this large data set.

Results

Bering Sea assemblage composition

A total of 21 species (Figure 2.3) were identified in the Bering Sea representing a mixture of Arctic and subarctic species. The dominant taxa identified were *Normanicythere leioderma*, *Sarsicytheridea bradii*, *Semicytherura complanata*, and *Pectocythere janae* (provisionally called *Kotoracythere arctoborealis*, per E. Schornikov and W. Briggs, Jr., personal communication). While varying from year-to-year, these four species cumulatively comprised 72% of all specimens identified. During the 34-year time span of this study, average ostracode density was 3.18 specimens per gram of dry sediment. The number of individuals fluctuated widely from sample to sample, from a few specimens to several hundred.

I performed a cluster analysis to sort species with similar patterns of abundance into separate groups (Figure 2.3). Using all samples (n=225), a dendrogram grouped the two most dominant species, *N. leioderma* and *S. bradii*, as a single separate node, based upon similar abundance patterns. Another cluster is linked from this one node to include a second grouping, which includes some euryhaline species, such as *Heterocyprideis fascis* and

Paracyprideis pseudopunctillata, *P. janae* and *Cytheromorpha macchesneyi* also grouped together. Finally, several relatively uncommon species clustered together including *Cytheropteron elaei* and *Robertsonites tuberculatus*.

Distributions of dominant taxa in the Arctic Ocean and North Pacific

The dominant taxa I found in the northern Bering Sea have been identified living in other areas of the Arctic, as well as subarctic and temperate regions. I used the ~700-sample Modern Arctic Ostracode Database (Cronin et al., 2010a; 2010b) collected over the past 50 years to provide some context for our collections. *N. leioderma*, *S. bradii* and *S. complanata* are typically circum-Arctic in distribution on continental shelves along the Chukchi-Beaufort and Laptev-Kara Sea margins (Figures 2.4A-C). The single most dominant species observed in all years in the northern Bering Sea (except 2004, where only limited samples were available) was *N. leioderma*. It also occurred with less frequency in the Chukchi-Beaufort Sea region at water depths of 10 to 80 m, comprising up to 30% of the ostracode fauna. *S. complanata* is relatively rare in the western Beaufort and Chukchi Sea and is more common along Siberian shelves (Stepanova et al., 2007). *S. bradii* occurred in the Chukchi and Beaufort Seas, usually comprising between 20-40% of the assemblage at depths of 0-50 m.

In contrast, *Pectocythere* is primarily a more temperate genus that inhabits

subarctic regions in the Pacific Ocean, such as the Gulf of Alaska (Brouwers, 1990). *P. janae* inhabits the Bering Sea in varying abundances depending on the year, occurring in higher abundances during relatively warmer temperatures. It has been reported in the high Arctic only in low numbers in a few samples in the western Beaufort Sea collected in 1969 and 1970 (Figure 2.4D) and in the East Siberian Sea in Chaunskaya Bight Inlet, a warm refugium inhabited by a number of species common to the Bering Sea (E. Schornikov, personal communication, 2012). *P. janae* is absent in other parts of the East Siberian Sea (E. Schornikov, personal communication, 2012). It has not been reported in the Laptev, Kara, Barents, Norwegian, or Greenland Seas. Although its precise temperature tolerance is not known, this species is clearly not a circum-Arctic, cryophilic species like others found in the Bering Sea assemblages, and is only found in the Bering and the Arctic (Chukchi-Beaufort and Eastern Siberian Seas) during periods with warmer water temperatures.

Temporal trends in Bering Sea indicator species

I plot the relative proportions (percent abundance of each species out of the total assemblage) for four key species for each year in which samples were available from 1976-2010 (Figures 2.5B-E). These abundance data were evaluated with respect to BWT and May SST (Figure 2.5A). Confidence limits

were generated using the binomial methods of Buzas (1990).

Normanicythere leioderma (Figure 2.5B) comprised 40-50% of the Bering assemblages in 1976-1977 before declining to 10% during warming in the late 1970s/early 1980s. *N. leioderma* increased in abundance during the 1980s and 1990s, peaking at >70% during the cold year of 1999. This species decreased to a minimum in the early 2000s, as temperatures warmed between 2000 and 2005 and then increased again in abundance during the cooler period since 2006.

Sarsicytheridea bradii (Figure 2.5C) comprised between 8 and 60% of Bering Sea ostracode assemblages from 1976 until 2002, followed by a sharp decline in 2003-2006, apparently in response to warmer temperatures. The decline, however, lagged the near-immediate decline of *N. leioderma* by a year or two.

Semicytherura complanata (Figure 2.5D) is in a genus that includes several related subspecies living in cold temperate to Arctic regions. Bering Sea populations of *S. complanata* comprised <10% of assemblages during the late 1970s through 1999, followed by an increase to 30 to 40% during 2004 to 2006.

In contrast to some of the cryophilic species discussed above, *P. janae* was typically absent to very rare (<4% of assemblages) in the northern Bering Sea

from 1976 through 1999 (Figure 2.6E). During the interval 2001 to 2006, it increased to 10 to 30% of northern Bering assemblages as water temperatures increased.

Canonical correspondence analysis for Bering Sea species

A canonical correspondence analysis (CCA) is a standard form of correspondence analysis that allows environmental data to be incorporated into the analysis. It was used to examine the frequencies of ostracode species in relation to several environmental variables that may influence their overall abundance (Figure 2.6; Park and Cohen, 2011; Torres Saldarriaga and Martínez, 2010). The five most abundant species were evaluated in the context of the following variables: 1) surface air temperature (SAT) in the Chirikov Basin (Z. Brown, personal communication); 2) SAT along the Inner Shelf (Z. Brown, personal communication); 3) the Arctic Oscillation Index (<http://www.beringclimate.noaa.gov/data/>); 4) May SST in the southeastern Bering Sea (<http://www.beringclimate.noaa.gov/data/>), and 5) the number of open water days in the Chirikov Basin and Inner Shelf (Brown et al., 2011). Only samples containing ≥ 20 total specimens ($n=77$) were used in this analysis (see Buzas, 1990). Considering that ostracode density was low (e.g. < 200 specimens per sample), which is typical on continental shelves, I decided that ≥ 20 specimens per sample would reflect the dominant species

living in the area. A higher minimum cutoff would have eliminated a significant number of sites and precluded a regional characterization. This threshold best balances the competing demands of representative population and geographic coverage. I recognize that due to the low number of specimens, not all the rare species may be found, but the number of sediment samples (n=77, 4923 specimens) in the study vicinity provides a reasonable validation of general community composition. The 1978 data were excluded because those samples were collected at extremely near shore sites having much lower salinity.

The CCA shows that the frequency of *P. janae* is associated with high SATs, indicating a distinct ecological niche for *P. janae* because of the high degree of separation within its own quadrant in the CCA plot. Samples from the year 2010 (maroon circles) are in the opposite quadrant from the SAT vectors and *P. janae*, consistent with colder water temperatures in 2010. Samples from 1994 (light gray circles) cluster together because in that year *S. bradii* and *N. leioderma* represented 36% and 49% of the total ostracode population, respectively. A few samples from 1977 and 1976 (pink and moss green circles) are located in lower salinity waters of Norton Sound and correspondingly group with *C. macchesneyi*, a species that can tolerate reduced salinity. Several samples in 2010 (maroon circles) contained higher proportions of *C. macchesneyi* as well. Data corresponding to *N. leioderma* is centrally distributed in the plot, meaning that it is abundant in most of the

samples in most of the years.

Chukchi Sea ostracode assemblages

In the Chukchi Sea, I identified a total of 28 species from 8 surface samples in 2009 and 8 samples in 2010, representing a mixture of Arctic and subarctic species (Figure 2.7). The most abundant species in the Chukchi Sea were *P. pseudopunctillata* (17% in 2009 and 16% in 2010) and *S. bradii* (27% in 2009 and 8.4% in 2010). Although the Chukchi shelf has many species in common with the Bering Sea, *N. leioderma* was much less abundant in the Chukchi (0.8% in 2009 and 11% in 2010); *P. janae* comprised 7.8% in 2009 and 5.1% in 2010. Ostracode density averaged 1.6 ostracodes per dry gram of sample.

Discussion

During the 34-year time span of this study, I found that two primary assemblages inhabited the northern Bering Sea. One assemblage is dominated by Arctic species (e.g. *N. leioderma*, *S. bradii*), and the other has greater proportions of temperate-subarctic species (e.g. *P. janae*). These two end members are evident during the relatively cool years 1994 and 1994 and warm years 2000-2006 (Figures 2.9A-D). These data suggest that *P. janae* and *S. complanata* prefer warmer conditions (Figure 2.8A-B). The CCA

(Figure 2.6) further suggests that *P. janae* has a distinctly warmer temperature preference, as it plots in its own quadrant and is positively correlated with sea-air temperatures. I hypothesize that *P. janae* migrates into the Bering Sea in greater numbers during these warm periods. Likewise, in the two years of Chukchi Sea assemblage data, *P. janae* was found in low abundance, which may further signify its range expansion. During 2004-2006, *S. complanata* reached a maximum of 40% abundance of the total ostracode population, suggesting a preference for warmer water and/or minimal sea ice (Figure 2.5C). In contrast, *N. leioderma* and *S. bradii* decline in abundance in warm years (Figures 2.8C-D). These patterns support prior studies that show water temperatures are critical for survival and reproduction in many marine ostracodes (Hazel, 1970; Brouwers et al., 1988).

This study also provides insight into the ostracode faunal composition of shallow, continental shelf areas in the Pacific subarctic and Arctic. The subarctic Bering Sea assemblage contains different dominant species than the Arctic assemblages in the Chukchi, Beaufort, Laptev and Kara Seas, which had many more species in common (See Chapter 1, Figure 1.5). The greater proportion of *N. leioderma* found in the Bering Sea is the key difference between subarctic and Arctic populations. Although Stepanova (2007) found this species in a few shallow samples in the Kara Sea, occurring at depths of less than 50m, *N. leioderma* is present outside the Arctic and prefers subarctic ecosystems. For example, it occurs in shallow coastal

waters of the Atlantic and Atlantic-influenced Arctic: Gulf of St. Lawrence (Norman, 1869), Iceland (Elofson, 1941), eastern Ellesmere Island (Brady and Norman, 1899), western Greenland (Stephensen, 1938), St. Margaret's Bay, Nova Scotia (Levings, 1975) and the Gulf of Maine (Blake, 1933). Hazel (1970) classified *N. leioderma* as an amphi-Atlantic species (i.e. a species that occurs on both eastern and western margins of the Atlantic) ranging in depth from 3 to 150 meters in the frigid-cold climate zone, which coincides with the Arctic-Nova Scotian biogeographic province. Hazel (1970) specifically noted that summer survival and reproductive temperatures control *N. leioderma*'s population. This agrees with our data showing a decline in *N. leioderma* during warmer periods in the northern Bering Sea.

Conclusions

This study provides the first faunal survey and time-series examination of ostracode assemblages in the Bering Sea. I conclude that the relative dominance of Arctic and subarctic species in the Bering Sea has changed during the last several decades as ocean temperatures fluctuated, illustrating the potential use of ostracodes to characterize ocean changes in the region. I hypothesize these faunal changes reflect either the direct effects of temperature or other temperature-related factors, such as reduced sea ice. Data collected from two research cruises on Chukchi Sea ostracodes are not

extensive enough to assess temporal change, but can serve as a baseline for future studies.

Table

Year	Month	Ship	Region
2010	March	<i>USCGC Polar Sea</i>	South of St. Lawrence Island
2009	March	<i>USCGC Healy</i>	South of St. Lawrence Island
2007	May-June	<i>USCGC Healy</i>	Chirikov and South of St. Lawrence Island
2006	May-June	<i>USCGC Healy</i>	Chirikov and South of St. Lawrence Island
2004	July	<i>CCGS Sir Wilfrid Laurier</i>	Chirikov and South of St. Lawrence Island
2003	July	<i>CCGS Sir Wilfrid Laurier</i>	Chirikov and South of St. Lawrence
2002	July	<i>CCGS Sir Wilfrid Laurier</i>	Chirikov and South of St. Lawrence
2001	July	<i>CCGS Sir Wilfrid Laurier</i>	Chirikov and South of St. Lawrence Island
1999	April	<i>USCGC Polar Sea</i>	South of St. Lawrence Island
1994	May-June	<i>RV Alpha Helix</i>	South of St. Lawrence Island
1990	June	<i>RV Alpha Helix</i>	South of St. Lawrence Island
1980	August	<i>Samuel Phillips Lee</i>	South of St. Lawrence Island
1978	Aug.-Sept.	<i>Sea Sounder</i>	Norton Sound, Bering
1978	July	<i>Karluk</i>	Norton Sound, Bering
1977	July-Aug.	<i>Sea Sounder</i>	Chirikov and Norton Sound
1976	March	<i>Sea Sounder</i>	Chirikov and Norton Sound
2009	July-Aug.	<i>RV Alpha Helix</i>	Chukchi
2010	July-Aug.	<i>RV Moana Wave</i>	Chukchi

Table 2.1. Listing of research cruises by year, month, ship, and region, from which samples for this study were collected.

Figures 2.1 – 2.8

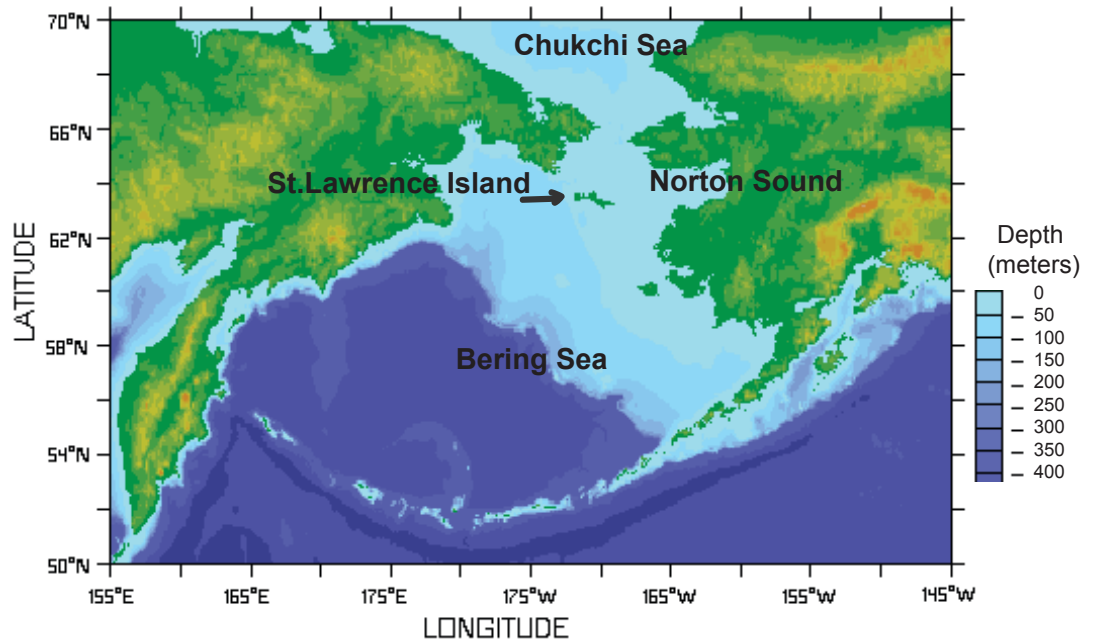


Figure 2.1. Bathymetry of the northern Bering and Chukchi Seas. Map legend does not show areas >400 m, such as the southwestern Aleutian Basin, which ranges from 400 to 3000 m.

Map derived from:

<http://www.pmel.noaa.gov/np/pages/seas/bseamap2.html>

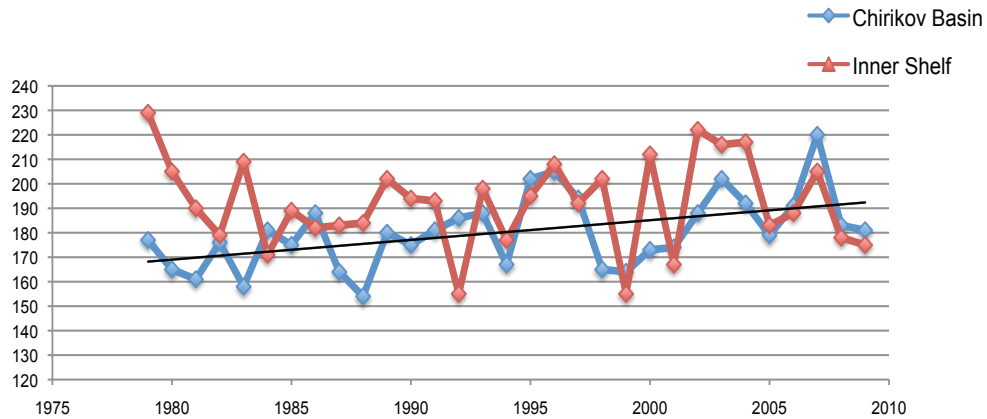


Figure 2.2. Number of open water days (reflecting length of ice-free period) in the Chirikov Basin and along the Inner Shelf, 1979-2009. Trend line shows open water duration in the Chirikov Basin (north of St. Lawrence Island) has increased over these three decades, accounting for an ice loss of $\sim 77 \pm 37 \text{ km}^2$ of ice per year, with ice exiting by mid-June (Brown et al., 2011). “Open water” is defined as a satellite-derived sea-ice concentration below 10%. The Inner shelf region (0–50 m depth) includes the Eastern shelf and the Gulf of Anadyr (bounded by Cape Navarin to the south, St. Lawrence Island to the east, and Cape Chukotskiy to the north); The Chirikov Basin region is bounded by St. Lawrence Island to the south, the Chukotka Peninsula to the west, Seward Peninsula to the east, and Bering Strait to the north.

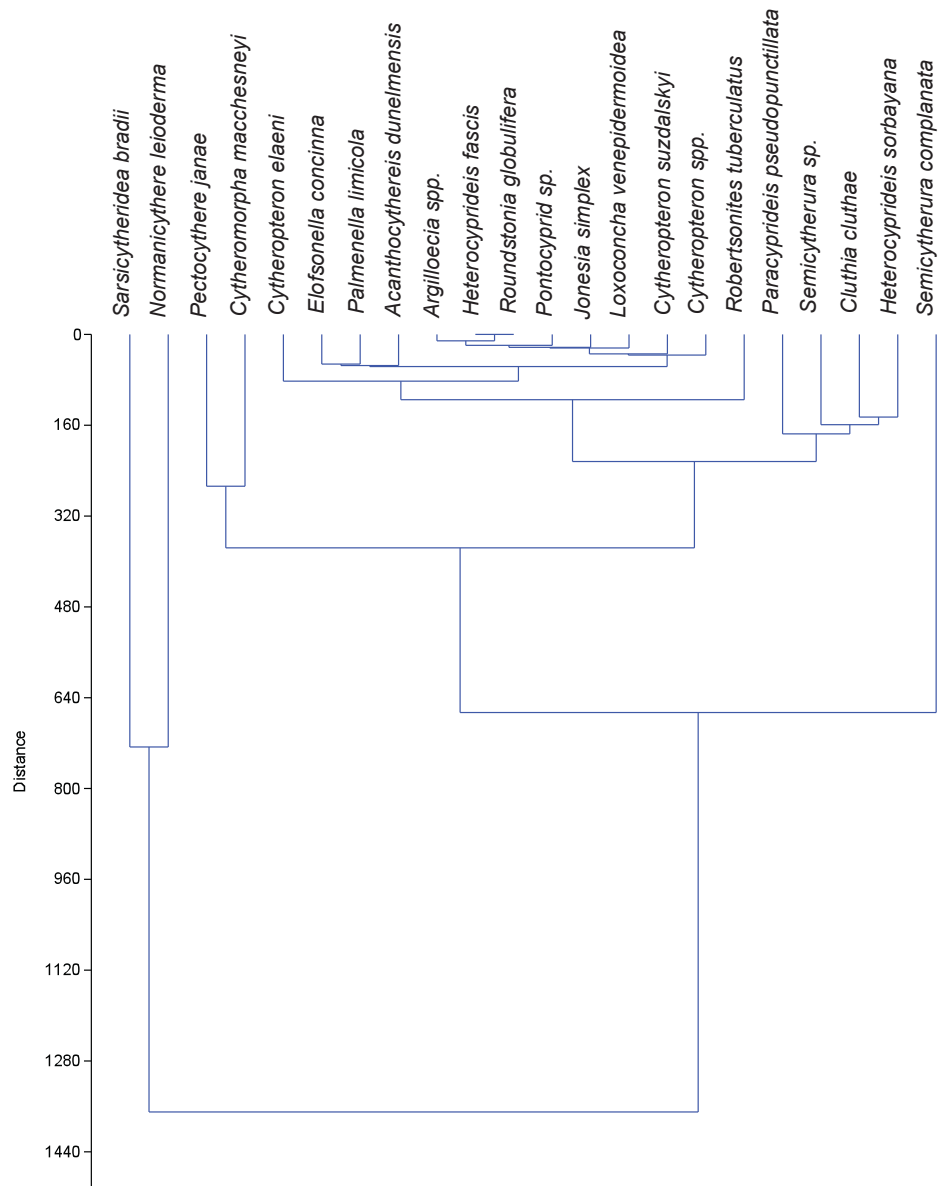
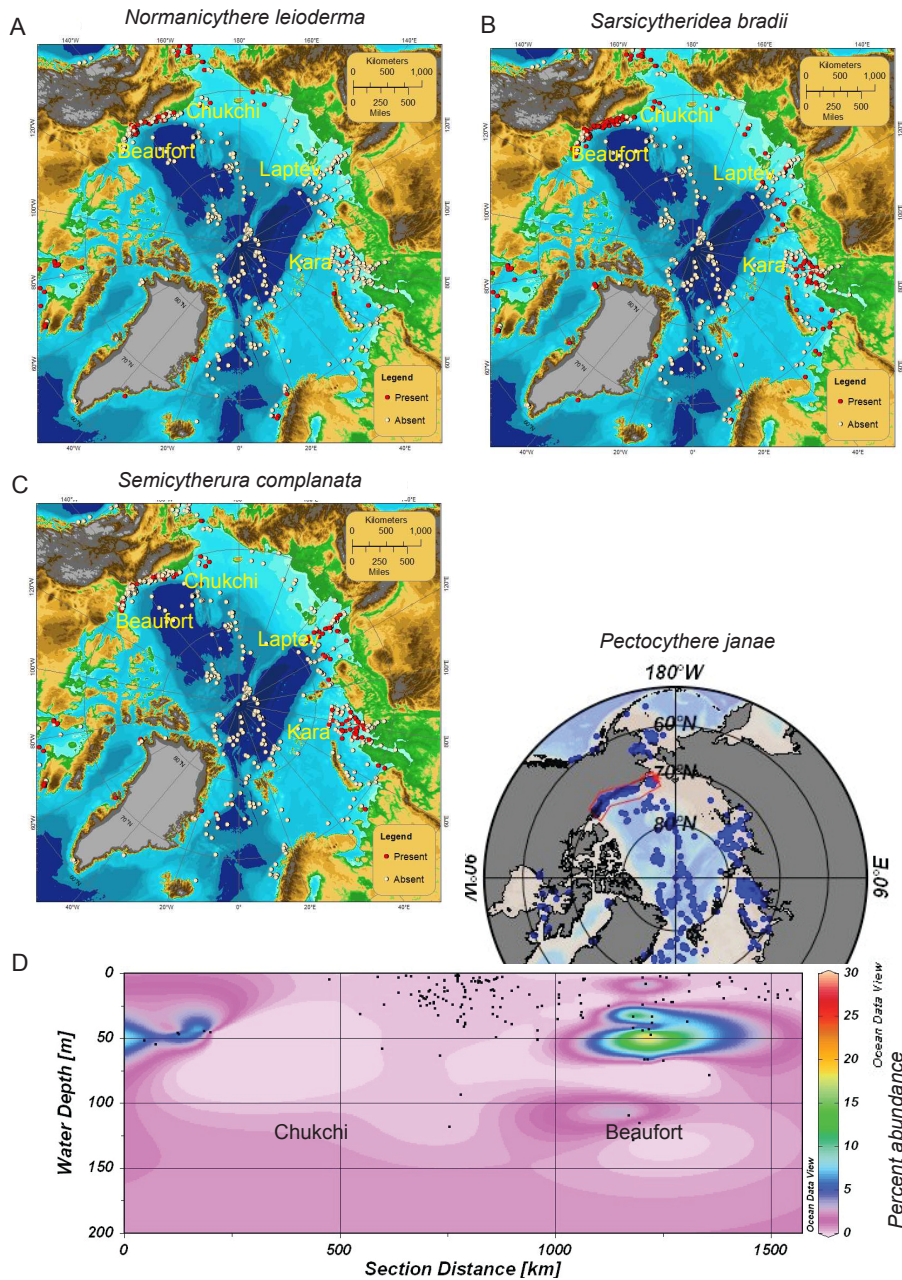


Figure 2.3. Cluster analysis with a Euclidean similarity measure of 21 species of ostracodes in the northern Bering Sea, 1976-2010. This grouping sorts species with similar patterns of abundance.



Figures 2.4A-C. Modern Arctic distribution and abundance of three key cryophilic species, *N. leioderma* (a), *S. bradji* (b), and *S. complanata* (c), based on a ~700-core-top sediment sample database (the Modern Arctic Ostracode Database, MAOD). The red circles indicate species presence, while the white circles indicate absence. The MAOD provides census data for approximately 100 species of benthic marine Ostracoda from modern surface sediments collected over the last 50 years from the Arctic Ocean and adjacent seas (Cronin et al., 2010).

Figure 2.4D. Contour plot of distribution, depth and abundance of *P. janae* along the red-outlined Chukchi/Beaufort Sea area. Transect runs from the Chukchi to the Beaufort Sea (left to right). From the MAOD 685-sample database, 140 samples (black circles) were analyzed for the abundance of *Pectocythere*. *P. janae* is rare along the Chukchi-Beaufort shelf, only appearing in 2 samples during 1969 and 1970 with an abundance of 5-18% of the sample's total ostracode population. It is absent along the Laptev-Kara shelf and is a more temperate Pacific species found in the Gulf of Alaska by Brouwers (1990).

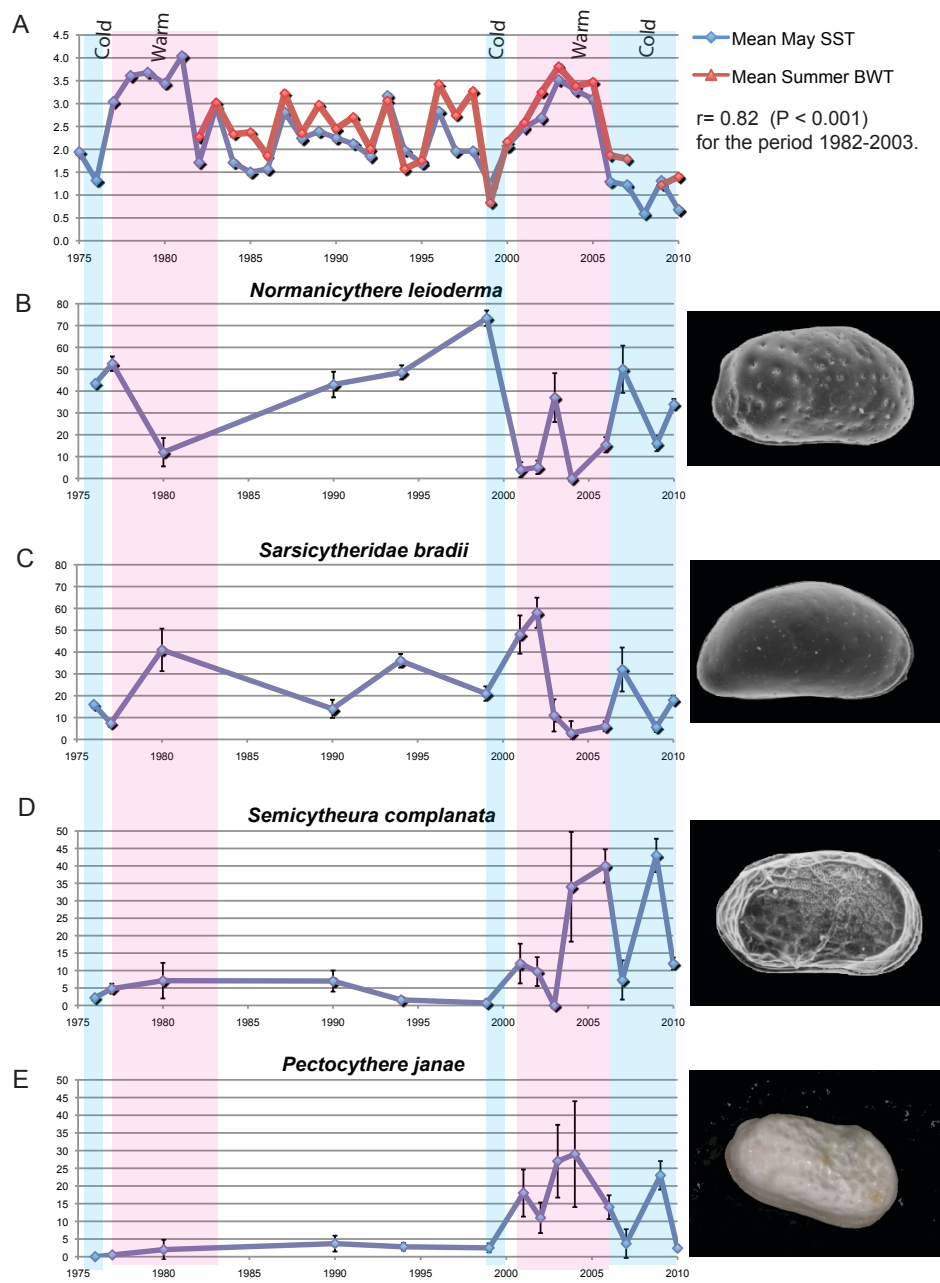
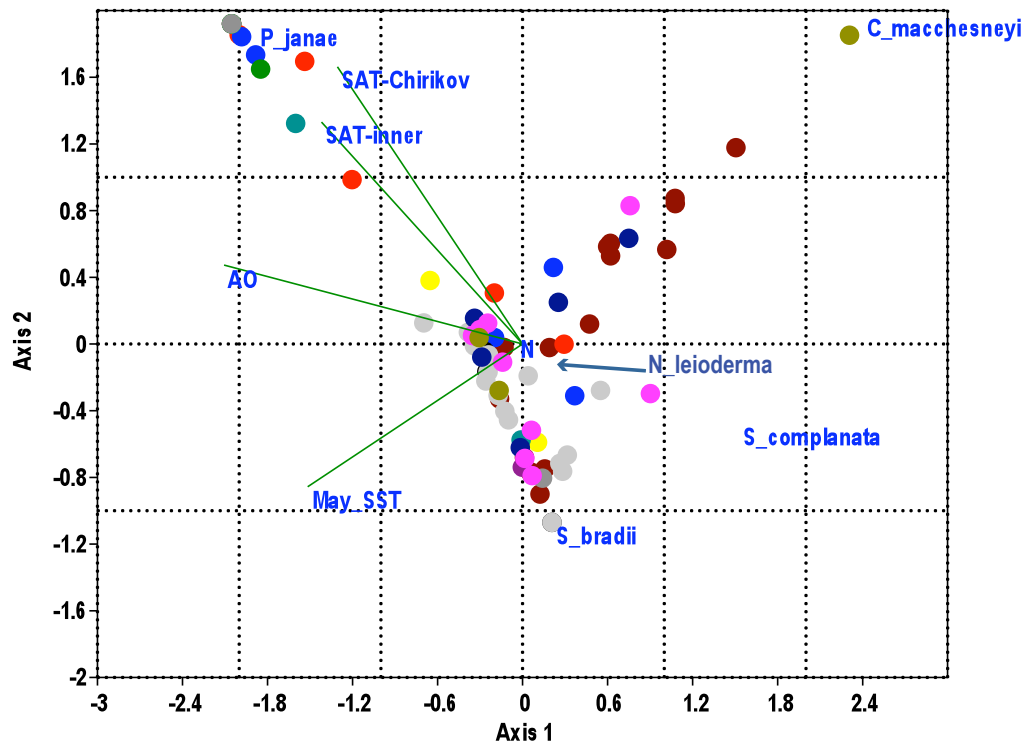


Figure 2.5A. Chirikov Basin and Inner Shelf mean summer sea-surface temperature (SST) from 1982 to 2009 (purple and green lines). In order to have a temperature record that encompassed the study's time period, we include May SST for the southeastern Bering since 1975 and summer BWT for the eastern Bering since 1982. Because the central-northern Bering Sea is shallow (<50m) and well mixed, SST and BWT patterns generally show broad decadal patterns but do not provide year- and site-specific temperature data for our exact study region or exact temperatures that ostracode species require. (Data from <http://www.beringclimate.noaa.gov/data/>)
Figures 2.5B-E. Plots of abundances of the four most common species in Bering Sea, 1976-2010. Results represent the relative abundance of the major taxa out of the entire population for each year. (Photos courtesy of A. Stepanova and 2.5E photo by L.Gemery)



Legend

- 2010 maroon ●
- 2009 red ●
- 2007 yellow ●
- 2006 blue ●
- 2004 green ●
- 2003 lime green ●
- 2002 teal ●
- 2001 gray ●
- 1999 black ●
- 1994 light gray ●
- 1990 navy ●
- 1980 purple ●
- 1977 pink ●
- 1976 moss green ●

Figure 2.6. Canonical correspondence analysis (CCA) results of five dominant ostracode species frequencies (n=77) in relation to several environmental variables (sea-air temperature [SAT] in the Chirikov Basin, SAT along the Inner Shelf, the Arctic Oscillation Index, May sea surface temperature [SST] in the southeastern Bering Sea) that may influence their overall abundance and distribution. The green vector lines show the environmental variables and the quadrant and samples with which they are associated. Although it is difficult to disentangle the independent effects of the variables, the CCA shows that *P. janae*'s ecology is distinct from the other dominant species and its frequency correlates with high SATs, indicating a warmer water affinity. Samples from the year 2010 (maroon circles) are in the opposite quadrant from the SAT vectors and *P. janae*, consistent with colder water temperatures in 2010. Samples from 1994 (light gray circles) cluster together indicating the dominance of *S. bradii* and *N. leioderma*, which, in that year, represented 36% and 49% of the total ostracode population, respectively. *C. macchesneyi*, a species that can tolerate reduced salinity, shows a correlation with a few samples from 1977 and 1976 (pink and moss green circles) that are located in lower salinity waters of Norton Sound. Samples from 2010 (maroon circles) also contained a higher percentage of *C. macchesneyi* compared to past years. Data corresponding to *N. leioderma* is centrally distributed in the plot, meaning that it is abundant in most of the samples in most of the years. According to the eigenvalues, axis one (80%) and axis two (15%) account for a combined 94% of the variance in this analysis.

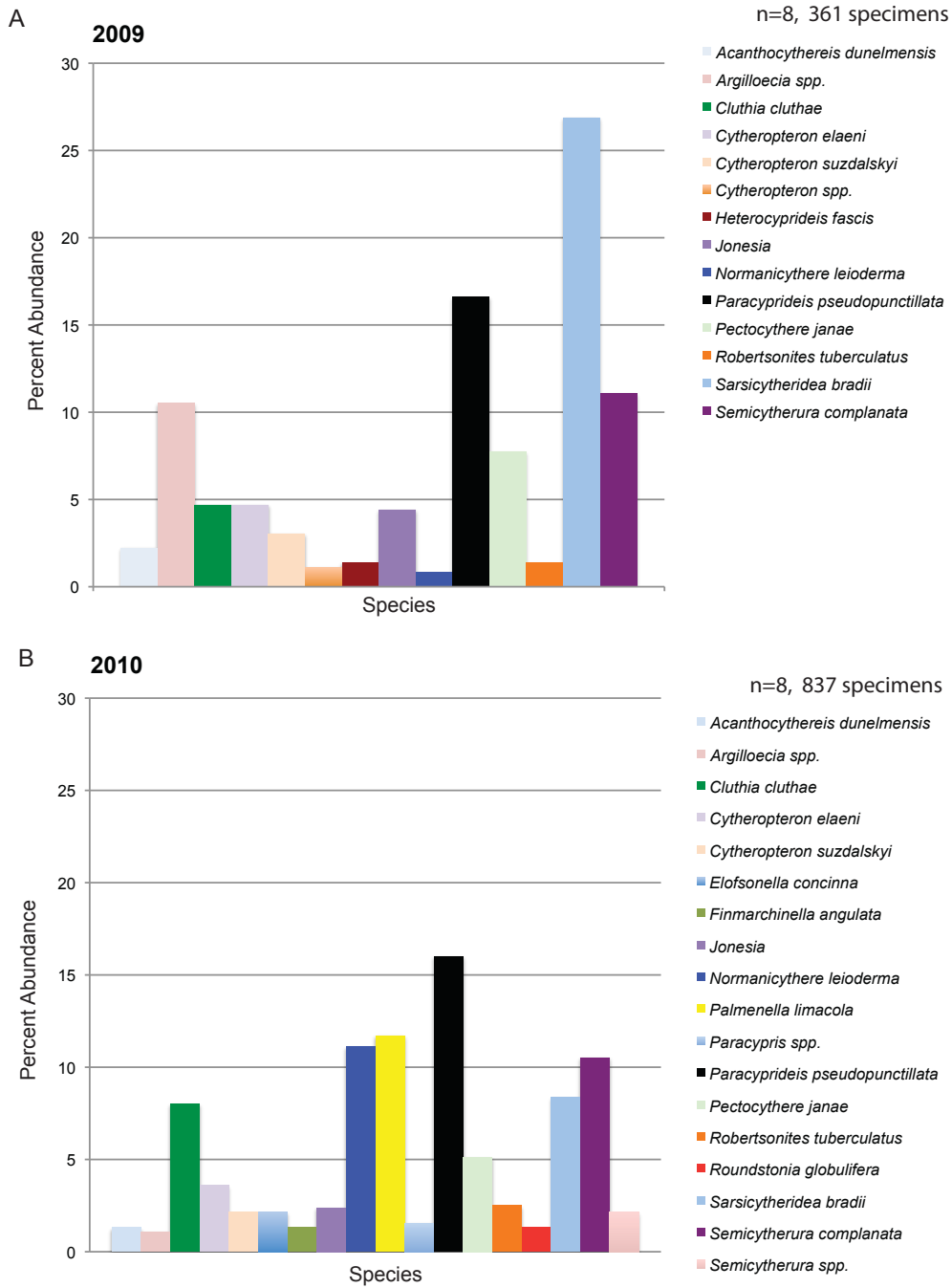


Figure 2.7. The Chukchi Sea ostracode species assemblages in 2009 and 2010. Bar plots include species that comprised >1% of the total species population. In 2009, eight samples yielded 361 ostracode specimens and in 2012, eight samples yielded 837 specimens.

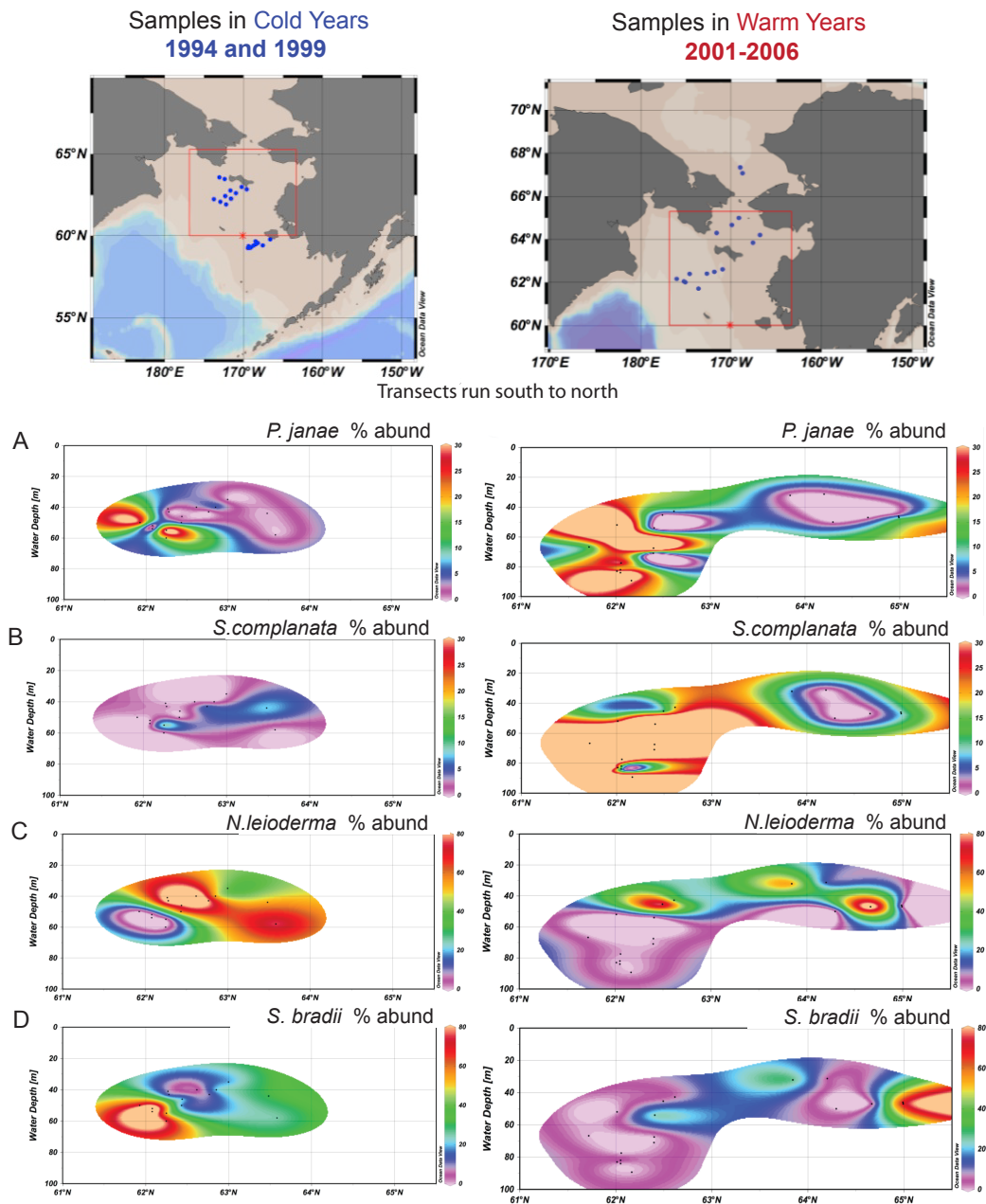


Figure 2.8A-D. Contour plots comparing species abundance in cold years (1994 and 1999) vs. warm years (2001-2006) north and south of St. Lawrence Island. Maps (top) show central-northern Bering shelf study area and locations of samples (blue dots) in the years represented. Contour plots show abundance of key taxa in south-north cross sections to depict the changes in major species abundance during these ocean-atmosphere shifts. Two assemblages are present; one dominated by Arctic species (*N. leioderma* and *S. bradii*) in colder years, another with significant numbers of more temperate species (*P. janae*) representing a mixture of Arctic and sub-Arctic species.

Appendices

Appendices 1A and 1B are attached separately as supplemental files.

References, Chapter 1

Arrigo, K. R., and G. L. van Dijken. 2011. Secular trends in Arctic Ocean net primary production. *J. Geophys. Res.* 116, C09011.

Belkin, I. M., P. C. Cornillon, and K. Sherman. 2009. Fronts in large marine ecosystems. *Prog. Ocean.* 81,1-4, 223-36.

Bluhm, B.A. and J.M. Grebmeier. 2011. Arctic Ocean Primary Productivity. In: Richter-Menge, J., M.O. Jeffries and J.E. Overland, Eds. *Arctic Report Card 2011*. http://www.arctic.noaa.gov/reportcard/biodiv_benthic_organisms.html

Bluhm, B., and R. Gradinger. 2008. Regional variability in food availability for Arctic marine mammals. *Ecol. Appl.* 18, S77–96.

Boomer, I and G. Eisenhauer. 2002. Ostracode faunas as palaeoenvironmental indicators in marginal marine environments. In: *The Ostracoda: Applications in Quaternary Research* (Eds: Holmes, J. A. and A.R. Chivas). Geophysical Monograph Series, Volume 131. American Geophysical Union, Washington, D.C.

Brouwers, E.M. 1994. Systematic paleontology of Quaternary ostracode assemblages from the Gulf of Alaska: Part 3. Family Cytheruridae. *U.S. Geol.*

Surv. Prof. Pap. No. 1544, 1–43.

Brouwers, E.M. 1993. Systematic paleontology of Quaternary ostracode assemblages from the Gulf of Alaska: Part 2. Families Trachyleberididae, Hemicytheridae, Loxoconchidae, Paracytheridae. *U.S. Geol. Surv. Prof. Pap.* No. 1531, 1–40.

Brouwers, E.M., N.O. Jorgensen, and T.M. Cronin. 1991. Climatic significance of the ostracode fauna from the Pliocene Kap Kobenhavn Formation, north Greenland. *Micropaleontology*. 37,3, 245-267.

Brouwers, E.M. 1990. Systematic Paleontology of Quaternary Ostracode Assemblages from the Gulf of Alaska: Part 1. Families Cytherellidae, Bairdiidae, Cytheridae, Leptocytheridae, Limnocytheridae, Eucytheridae, Krithidae, Cushmanideidae. *U.S. Geol. Surv. Prof. Pap.* No. 1510, 1–40.

Brouwers, E.M. 1988a. Palaeobathymetry on the continental shelf based on examples using ostracods from the Gulf of Alaska. In: *Ostracoda in the Earth Sciences* (Eds: DeDecker, P., Colin, J.P., Peypouquet). Elsevier, 55-76.

Brouwers, E.M. 1988b. Sediment transport detected from the analysis of ostracod population structure; An example from the Alaskan continental shelf. In: *Ostracoda in the Earth Sciences* (Eds: DeDecker, P., Colin, J.P.,

Peypouquet). Elsevier, 231-244.

Brown, Z.W., G.L. van Dijken, and K.R. Arrigo. 2011. A reassessment of primary production and environmental change in the Bering Sea. *J. Geophys. Res.* 116, C08014.

Clark, D.L., L.A. Chern, J.A. Hogler, C.M. Mennicke, and E.D. Atkins. 1990. Late Neogene climate evolution of the central Arctic Ocean. *Mar. Geol.* 93, 69-94.

Cooper, L.W., M. Janout, K.E. Frey, R. Pirtle-Levy, M.L. Guarinello, J.M. Grebmeier, J.R. Lovvorn. 2012. The relationship between sea ice break-up, water mass variation, chlorophyll biomass, and sedimentation in the northern Bering Sea. *Deep Sea Res., II*. In press. doi:10.1016/j.dsr2.2012.02.002

Cronin, T. M., L.J. Gemery, E. M. Brouwers, W. M. Briggs, Jr., A. Wood, A. Stepanova, E. I. Schornikov, J. Farmer, K. E. S. Smith. 2010a. Arctic Ostracodes Database-2010. IGBP PAGES/World Data Center-A for Paleoclimatology Data Contribution Series # 95-023. NOAA/NGDC Paleoclimatology Program, Boulder CO, USA.
(ftp://ftp.ncdc.noaa.gov/pub/data/paleo/contributions_by_author/cronin2010/cronin2010.txt)

Cronin, T.M., Gemery, L., Briggs Jr., W.M., Jakobsson, M., Polyak, L. and Brouwers, E.M. 2010b. Quaternary sea-ice history in the Arctic Ocean based on a new ostracode sea-ice proxy. *Quat. Sci. Rev.* 05.024.

Cronin, T.M., H.J. Dowsett, G.S. Dwyer, P.A. Baker, and M.A. Chandler. 2005. Mid-Pliocene deep-sea bottom-water temperatures based on ostracode Mg/Ca ratios. *Mar. Micropaleontol.* 54, 249-261.

Cronin, T.M. and Vann. 2003. The sedimentary record of climatic and anthropogenic influence on the Patuxent estuary and Chesapeake Bay ecosystems. *Estuaries.* 26, 196–209.

Cronin, T.M., M.E. Raymo, K.P. Kyle. 1996. Pliocene (3.2–2.4 Ma) ostracode faunal cycles and deep ocean circulation, North Atlantic Ocean. *Geology.* 24, 695–698.

Cronin, T.M., T.R. Holtz, and R.C. Whatley. 1994. Quaternary paleoceanography of the deep Arctic Ocean based on quantitative analysis of Ostracoda. *Mar. Geol.* 119, 3-4, 305-332.

Cronin, T. M., R. Whatley, A. Wood, A. Tsukagoshi, N. Ikeya, E. M. Brouwers, and W. M. Briggs Jr. 1993. Microfaunal evidence for elevated Pliocene temperatures in the Arctic Ocean. *Paleoceanography.* 8, 2, 61–173.

Cronin, T.M. 1988. Paleozoogeography of postglacial ostracoda from northeastern North America. In: N.R. Gadd, Ed. *The Late Quaternary development of the Champlain Sea Basin*. Geological Association of Canada Special Paper. 35, 125-144.

Cronin, T.M. 1981. Paleoclimatic implications of Late Pleistocene marine ostracodes from the St. Lawrence Lowlands. *Micropaleontology*. 27,4, 383-418.

Didié, C. and H.A. Bauch. 2000. Species composition and glacial-interglacial variations in the ostracode fauna of the northeast Atlantic during the past 200,000 years. *Mar. Micropaleontol.* 40, 105–129.

Elofson, O. 1941. Zur Kenntnis der marinen Ostracoden Schwedens mit besonderer Berücksichtigung der Skageraks. *Zoologiska Bidrag fran Uppsala* 19, 217–534.

Frey, K.W., K.R. Arrigo and R.R. Gradinger. 2011. Arctic Ocean primary productivity. In: Richter-Menge, J., M.O. Jeffries and J.E. Overland, Eds. *Arctic Report Card 2011*.

http://www.arctic.noaa.gov/reportcard/primary_productivity.html

Gaston, K.J. 2000. Global patterns in biodiversity. *Nature*. 405, 220- 227.

Grebmeier J.M. 2012. Shifting patterns of life in the Pacific Arctic and Sub-Arctic seas. *Ann. Rev. Mar. Sci.* 4, 63-78.

Grebmeier, J.M., L.W. Cooper, and S.E. Moore. 2011. Marine ecology: Biological responses to changing sea ice and hydrographic conditions in the Pacific Arctic Region. In: Richter-Menge, J., M.O. Jeffries and J.E. Overland, Eds. *Arctic Report Card 2011*.

http://www.arctic.noaa.gov/reportcard/pacific_arctic.html

Grebmeier, J. M., S.E. Moore, J.E. Overland, K.E. Frey, and R.R. Gradinger, 2010. Biological response to recent Pacific Arctic sea-ice retreats. *EOS Trans. AGU*. 91, 18.

Grebmeier, J.M., J.E. Overland, S.E. Moore, E.V. Farley, E. C. Carmack, L.W. Cooper, K.E. Frey, J. H. Helle, F. A. McLaughlin, and S.L. McNutt. 2006a. A major ecosystem shift in the northern Bering Sea. *Science*. 311, 1461–1464.

Grebmeier, J.M., L.W. Cooper, H.M. Feder and B.I. Sirenko. 2006b. Ecosystem dynamics of the Pacific-influenced North Bering and Chukchi Seas in the Amerasian Arctic. *Prog. Oceanogr.* 71, 331-361.

Hammer, Ø., Harper, D.A.T., and P. D. Ryan. 2001. PAST: Paleontological Statistics Software Package for Education and Data Analysis. *Palaeontologia Electronica*. 4,1, 9pp.

http://palaeo-electronica.org/2001_1/past/issue1_01.htm

Hare, S.R. and N.J. Mantua. 2000. Empirical evidence for North Pacific regime shifts in 1977 and 1989. *Prog. Oceanogr.* 47, 103-145.

Hartmann, G. 1992. Zur Kenntnis der rezenten und subfossilen Ostracoden des Liefdefjords (Nordspitzbergen, Svalbard).i.teil. Mit einer tabelle subfossil nachgewiesener Foraminiferen. *Mitt. hamb. zool. Mus. Inst.* 89, 181-225.

Hazel, J.E. 1970. Atlantic Continental Shelf and Slope of United States—Ostracode Zoogeography in The Southern Nova Scotian and Northern Virginian Faunal Provinces. *U.S. Geol. Surv. Prof. Pap.* No. 529-E, E1–E21.

Herman, P.M.J., J.J. Middelburg, J. van de Koppel, C.H.R. Heip. 1999. Ecology of estuarine macrobenthos. *Adv. Ecol. Res.* 29:195–240.

Horne, D.J., A. Cohen and K. Martens. 2002. Taxonomy, morphology and biology of Quaternary and Living Ostracoda. In: *The Ostracoda: Applications in Quaternary Research* (Eds: Holmes, J. A. and A.R. Chivas). Geophysical

Monograph Series, 131, American Geophysical Union, Washington, D.C., 5-36.

Hunt, G. L., and P. Stabeno. 2002. Climate change and control of energy flow in the southeastern Bering Sea. *Prog. Oceanogr.* 55, 5–22.

Hunt, G.L., P. Stabeno, G. Walters, E. Sinclair, R.D. Brodeur, J.M. Napp, and N.A. Bond. 2002. Climate change and control of the southeastern Bering Sea pelagic ecosystem. *Deep-Sea Res. II.* 49, 5821-5853.

Joy, J.A., and D.L. Clark. 1977. The distribution, ecology and systematics of the benthic Ostracoda of the central Arctic Ocean. *Micropaleontology.* 23, 129-154.

Lee, S.H., H.M. Joo, M.S. Yun and T.E. Whitley. 2011. Recent phytoplankton productivity of the northern Bering Sea in 2007. *Pol. Bio.* 35,1, 83-98.

Mueter, Franz J., and M.A. Litzow. 2008. Sea ice retreat alters the biogeography of the Bering Sea Continental Shelf. *Eco. App.* 18, 309–320.

Neale, J.W., and H.V. Howe. 1975. The marine Ostracoda of Russian Harbour, Novaya Zemlya and other high latitude faunas. *Bull. Am. Paleo.* 65,

381-431.

Park, L.E. and A.S. Cohen. 2011. Paleocological response of ostracods to early Late Pleistocene lake-level changes in Lake Malawi, East Africa.

Palaeogeogr., Palaeoclimatol., Palaeoecol. 303, 71–80.

Penney, D.N. 1989. Recent shallow marine Ostracoda of the Ikerssuak (Bredefjord) district, Southwest Greenland. *J. Micropalaeo.* 8, 55-75.

Polyakov, I.V., V.A. Alexeev, I. M. Ashik, S. Bacon, A. Beszczynska-Möller, E.

C. Carmack, W. Walczowski , and R. Woodgate. 2011. Fate of early 2000s Arctic warm pulse. *Bull. Am. Meteorol. Soc.* 92, 561–566.

Radi, T. and A. de Vernal. 2008 Dinocysts as proxy of primary productivity in mid-high latitudes of the Northern Hemisphere. *Mar. Micropaleontol.* 68, 84–114.

Sars, G.O. 1866. Oversigt af Norges marine Ostracoder: Vidensk. -Selsk. Forhandl. Christiania. 17 (for 1865), 1-130.

Sars, G.O. 1922-1928. An account of the Crustacea of Norway Volume IX, Ostracoda: Bergen Museum, Bergen, Norway.

Schornikov, E.I. and M.A. Zenina. 2006. Benthic ostracod fauna of the Kara, Laptev and East-Siberian seas (data from the expeditions carried out by the Pacific Oceanography Institute of the Eastern Branch of the Russian Academy of Sciences). Proceedings of the Arctic regional center. vol. IV, p. 156-211. Izd. Dalnauka, Vladivostok (in Russian).

Smith, A.J. and D.J. Horne. 2002. Ecology of Marine, Marginal Marine and Nonmarine Ostracodes. In: Holmes, J. A. and A.R. Chivas, (Eds.), *The Ostracoda: Applications in Quaternary Research*. Geophysical Monograph Series, Volume 131. American Geophysical Union, Washington, D.C.

Springer, A.M., C.P. McRoy, M.V. Flint. 1996. The Bering Sea green belt: shelf-edge processes and ecosystem production. *Fish. Oceanogr.* 5, 205–223.

Springer, A.M. and C.P. McRoy. 1993. The paradox of pelagic food webs in the northern Bering Sea—III. Patterns of primary production. *Cont. Shelf Res.* 13, 5–6, 575-599.

Steele M., W. Ermold, J. Zhang. 2008. Arctic Ocean surface warming trends over the past 100 years. *Geophys. Res. Lett.* 35, L02614.

Steineck, P.L. D. Dahler, E.M. Hoose and D. McCalla. 1985. Oligocene to

Quaternary ostracods of the central equatorial Pacific (Leg 85, DSDP-IODP).
In: Hanai, T., N. Ikeya, K. Ishizaki, (Eds.), *Evolutionary Biology of Ostracoda: Its Fundamentals and Applications*, Proceedings of the Ninth International Symposium on Ostracoda.

Stepanova, A. Y., E.E. Taldenkova, and H.A. Bauch. 2010. Arctic Quaternary ostracods and their use in paleoreconstructions. *Paleo J.* 44, 1, 41–48.

Stepanova, A. Y., E.E. Taldenkova, and H.A. Bauch. 2007. Comparison study of the modern ostracod associations in the Kara and Laptev seas: Ecological aspects. *Mar. Micropaleontol.* 63, 111-142.

Stepanova, A. Yu. 2006. Late Pleistocene-Holocene and recent ostracoda of the Laptev Sea. Monograph. Suppl. Issue Russ. *Paleo J.* 40, 2, S91-S204.

Stepanova, A., E. Taldenkova, and H.A. Bauch. 2004. Ostracod species of the genus *Cytheropteron* from late Pleistocene, Holocene and recent sediments of the Laptev Sea (Arctic Siberia). *Revista Espanola de Micropaleontologia.* 36, 83-108.

Stepanova, A. Y., E.E. Taldenkova, and H.A. Bauch. 2003. Recent ostracoda from the Laptev Sea (Arctic Siberia): Species assemblages and some environmental relationships. *Mar. Micropaleontol.* 48, 23-48.

Stroeve, J.C., M.C. Serreze, S. Drobot, S. Gearheard, M.M. Holland, J. Maslanik, W. Meier, T. Scambos, 2008. Arctic sea ice extent plummets in 2007. *EOS Trans. AGU.* 89, 13-20.

Valentine, P.C. 1976. Zoogeography of Holocene ostracoda off Western North America and paleoclimatic implications. *U.S. Geol. Surv. Prof. Pap.* No. 916, 1–47.

Wang, M., J.E. Overland, P. Stabeno. 2012. Future climate of the Bering and Chukchi Seas projected by global climate models, *Deep Sea Res. II: Top. Stud. Oceanogr.* In press.

Whatley, R.C. 1982. Littoral and sublittoral Ostracoda from Sisimiut, West Greenland. In: Fox, A.D., and D.A. Stroud. Report of the 1979 Greenland White-Fronted Goose Study Expedition to Equalunqmiut Nunat, Western Greenland. University of Wales Press.

Whatley, R.C., and G. Coles. 1987. The late Miocene to Quaternary ostracoda of Leg 94, Deep Sea Drilling Project. *Revista Espanola de Micropaleontologia.* 19, 1, 33-97.

Woodgate, R. A., T. Weingartner, and R. Lindsay. 2010. The 2007 Bering

Strait oceanic heat flux and anomalous Arctic sea-ice retreat. *Geophys. Res. Lett.* 37, L01602.

Yasuhara, M., G. Hunt, G., T.M. Cronin, N. Hokenishi, H. Kawahata, A. Tsujimoto, M. Ishitake. 2012a. Climatic forcing of Quaternary deep-sea benthic communities in the North Pacific Ocean. *Paleobiology*. 38, 162–179.

Yasuhara, M., G. Hunt, G. van Dijken, K.R. Arrigo, T.M. Cronin, and J.E. Wollenburg. 2012b. Patterns and controlling factors of species diversity in the Arctic Ocean. *J. Biogeo.* In press.

Yasuhara, M., G. Hunt, T.M. Cronin, and H. Okahashi. 2009. Temporal latitudinal-gradient dynamics and tropical instability of deep-sea species diversity. *PNAS*. 106, 21717–21720.

References, Chapter 2

Arrigo, K.R., G. van Dijken, and S. Pabi. 2008. Impact of a shrinking Arctic ice cover on marine primary production. *Geophys. Res. Lett.* 35, L19603.

Belkin, I.M., P.C. Cornillon, and K. Sherman. 2009. Fronts in Large Marine Ecosystems. *Prog. Oceanogr.* 81, 223-236.

Blake, C. 1933. The Mount Desert region Ostracoda. In: Biological Survey of the Mount Desert Region. Wistar Institute of Anatomy and Biology. Philadelphia. pp. 229-41.

Brady, G. S. and A.M. Norman. 1896. A monograph of the marine and freshwater Ostracoda of the North Atlantic and of Northwestern Europe. Sections 2-4: Myodocopa, Cladocopa, Platycopa. *Sci. Trans. R. Dublin Soc.* Series 2, 5, 353-374.

Brown, Z.W., G.L. van Dijken, and K.R. Arrigo. 2011. A reassessment of primary production and environmental change in the Bering Sea. *J. Geophys. Res.* 116, C08014.

Brouwers, E.M. 1994. Systematic Paleontology of Quaternary Ostracode Assemblages from the Gulf of Alaska: Part 3. Family Cytheruridae. *U.S. Geol. Surv. Prof. Pap.* No. 1544, 1-43.

Brouwers, E.M. 1993. Systematic Paleontology of Quaternary Ostracode Assemblages from the Gulf of Alaska: Part 2. Families Trachyleberididae, Hemicytheridae, Loxoconchidae, Paracytheridae. *U.S. Geol. Surv. Prof. Pap.*

No. 1531, 1–40.

Brouwers, E.M. 1990. Systematic Paleontology of Quaternary Ostracode Assemblages from the Gulf of Alaska: Part 1. Families Cytherellidae, Bairdiidae, Cytheridae, Leptocytheridae, Limnocytheridae, Eucytheridae, Krithidae, Cushmanideidae. *U.S. Geol. Surv. Prof. Pap.* No. 1510, 1–40.

Brouwers, E.M. 1988. Palaeobathymetry on the Continental Shelf based on Examples using Ostracods from the Gulf of Alaska, In: *Ostracoda in the Earth Sciences* (Eds: DeDecker, P., J.-P. Colin, J.P., Peypouquet). Elsevier, pp. 55-76.

Buzas, M. 1990. Another Look at Confidence Limits for Species Proportions. *J. Paleo.* 64,5, 842-843.

Cronin, T.M., L.J. Gemery, W.M. Briggs Jr., M. Jakobsson, L. Polyak, and E.M. Brouwers. 2010a. Quaternary Sea-ice history in the Arctic Ocean based on a new Ostracode sea-ice proxy. *Quat. Sci. Rev.* 29, 25-26, 3349-3429.

Cronin, T.M., L. Gemery, E.M. Brouwers, W.M. Briggs, Jr., A. Wood, A. Stepanova, E.I. Schornikov, J. Farmer, and K.E.S. Smith. 2010b. Modern Arctic Ostracode Database. IGBP PAGES/WDCA Contribution Series Number: 2010-081.

ftp://ftp.ncdc.noaa.gov/pub/data/paleo/contributions_by_author/cronin2010/cronin2010.txt.

Elofson, O. 1941. Zur Kenntnis der marinen Ostracoden Schwedens, mit besonderer Berücksichtigung des Skagerraks. *Zoologiska Bidrag från Uppsala.* 19, 215-534.

- Grebmeier, J. M. 2012. Shifting patterns of life in the Pacific Arctic and Sub-Arctic seas. *Ann. Rev. Mar. Sci.* 4, 16, 1-16.
- Grebmeier, J. M., S.E. Moore, J.E. Overland, K.E. Frey, and R.R. Gradinger. 2010. Biological response to recent Pacific Arctic sea-ice retreats. *EOS Trans. AGU.* 91, 18.
- Grebmeier, J.M., J.E. Overland, S.E. Moore, E.V. Farley, E. C. Carmack, L.W. Cooper, K.E. Frey, J. H. Helle, F. A. McLaughlin, and S.L. McNutt. 2006a. A major ecosystem shift in the northern Bering Sea. *Science.* 311, 1461–1464.
- Grebmeier, J.M., L.W. Cooper, H.M. Feder and B.I. Sirenko. 2006b. Ecosystem dynamics of the Pacific-influenced North Bering and Chukchi Seas in the Amerasian Arctic. *Prog. Oceanogr.* 71, 331-361.
- Hammer, Ø., D.A.T. Harper and P. D. Ryan. 2001. PAST: Paleontological Statistics Software Package for Education and Data Analysis. *Palaeontologia Electronica.* 4,1, 9pp. http://palaeoelectronica.org/2001_1/past/issue1_01.htm
- Hazel, J.E. 1970. Atlantic Continental Shelf and Slope of United States—Ostracode Zoogeography in the Southern Nova Scotian and Northern Virginian Faunal Provinces. *U.S. Geol. Surv. Prof. Pap.* No. 529-E, E1–E21.
- Hunt, G.L. and P.J. Stabeno. 2002. Climate change and the control of energy flow in the southeastern Bering Sea. *Prog. Oceanogr.* 55, 1–2, 5–22.
- Hutchins, L.W. 1947. The bases for temperature zonation in geographical distribution. *Ecol. Monogr.* 17, 325-335.

Imbrie, J. and N.G. Kipp. 1971. A new micropaleontological method for quantitative paleoclimatology: application to a Late Pleistocene Caribbean core. In: *The Late Cenozoic Glacial Ages* (Ed: K.K. Turekian). Yale University Press, New Haven. pp. 77-181.

Joy, J.J. and D.L. Clark, 1977. The Distribution, Ecology and Systematics of the Benthic Ostracoda of the Central Arctic Ocean. *Micropaleo.* 23, 2, 129-154.

Kalnay, E., M. Kanamitsu, R. Kistler, W. Collins, D. Deaven, L. Gandin, M. Iredell, S. Saha, G. White, J. Woollen, Y. Zhu, A. Leetmaa, and R. Reynolds. 1996. The NCEP/NCAR 40-year reanalysis project. *Bull. Amer. Meteor. Soc.* 77, 437-471.

Levings, Coli N. D. 1975. Analyses of temporal variation in the structure of a shallow-water benthic community in Nova Scotia. *Intern. Revue Hydrobiol. Hydrogr.* 60, 4, 1522-2632.

Mantua, N.J. and S.R. Hare. 2002. The Pacific Decadal Oscillation. *J. Oceanogr.* 58, 1, 35-44.

Mueter, F.J. and M.A. Litzow. 2008. Sea ice retreat alters biogeography of the Bering Sea Continental Shelf. *Ecol. Appl.* 18, 309-320.

National Research Council. 1996. *The Bering Sea Ecosystem*. National Academy Press, Washington, D.C. 324pp.

Norman, A.M. 1869. *Shetland final dredging report, Pt. II on the Crustacea, Tunicata, Polyzoa, Echinodermata, Actinozoa, Hydrozoa & Porifera*. Rep. Brit. Ass. 38. Norwich, 247-336, Supplement pp. 341-2 [Ostracoda pp. 289-95].

Overland, J. E., M. Wang, and S. Salo. 2008. The recent Arctic warm period. *Tellus*. 60A, 589–597.

Park, L.E. and A.S. Cohen, 2011. Paleoeological response of ostracods to early Late Pleistocene lake-level changes in Lake Malawi, East Africa. *Palaeogeogr., Palaeoclim., Palaeoecol.* 303, 71–80.

Serreze, M.C., M.M. Holland, and J. Stroeve. 2007. Perspectives on the Arctic's shrinking sea-ice cover. *Science*. 315, 1533-1536.

Smith, A.J. and D.J. Horne. 2002. Ecology of Marine, Marginal Marine and Non-marine Ostracodes. In: *The Ostracoda: Applications in Quaternary Research* (Eds: Holmes, J. A. and A.R. Chivas). Geophy. Mono. Ser. Volume 131. American Geophysical Union, Washington, D.C. pp.37-64.

Stabeno, P.J., N.A. Bond, and S.A. Salo. 2007. On the recent warming of the southeastern Bering Sea Shelf. *Deep-Sea Res. II*. 54, 2599-2618.

Stephensen, K. 1938. Marine Ostracoda and Cladocera. In: *Zoology of Iceland III*. Copenhagen and Reykjavik, pp.1-19.

Stepanova, A. Y., E.E. Taldenkova, and H.A. Bauch. 2010. Arctic Quaternary ostracods and their use in paleoreconstructions. *Paleont. J.* 44, 1, 41–48.

Stepanova, A. Y., E.E. Taldenkova, and H.A. Bauch. 2007. Comparison study of the modern ostracod associations in the Kara and Laptev Seas: Ecological aspects. *Mar. Micropaleo.* 63, 111-142.

Stroeve, J.C., M.C. Serreze, S. Drobot, S. Gearheard, M.M. Holland, J.

Maslanik, W. Meier, and T. Scambos. 2008. Arctic sea ice extent plummets in 2007. *EOS Trans. AGU.* 89, 13-20.

Torres Saldarriaga, A. and J. I. Martínez. 2010. Ecology of non-marine ostracoda from La Fe reservoir (El Retiro, Antioquia) and their potential application in paleoenvironmental studies. *Rev. Acad. Col. Cienc.* 34, 132, 397-409.

Wang M., and J.E. Overland. 2009. A sea-ice free summer Arctic within 30 years? *Geophys. Res. Lett.* 36, L07502.